

**TWO-PHASE NUMERICAL SIMULATION OF NANOFUID  
LAMINAR CONVECTION HEAT TRANSFER THROUGH  
FLAT-PLATE SOLAR COLLECTOR**

Submitted in partial fulfillment of the requirement for the degree of

Bachelor of Science

In

Mechanical Engineering

Submitted by

**ABDUL ARIF**

Student No: 091436

Under the supervision of

**Dr. A. K. M. SADRUL ISLAM**

Professor

Department of Mechanical and Chemical Engineering (MCE)



**Islamic University of Technology (IUT)**

**The Organization of Islamic Cooperation (OIC)**

# **DECLARATION**

I hereby declare that thesis entitled “ Two-phase numerical simulation of nanofluid laminar convection heat transfer through a flat plate solar collector ” is an authentic report of my study carried out as requirements for the award of degree B.Sc (Mechanical Engineering) at Islamic University of Technology, Gazipur, Dhaka. Under the supervision of Dr. A. K. M. SADRUL ISLAM, Professor, Department of Mechanical and Chemical Engineering, IUT, during January 2013 to October 2013.

The matter embodied in this thesis has not submitted in part or full to any other institute for the award of any degree.

**Date :**

---

**ABDUL ARIF**  
St. No. 091436

This is to certify that the above statement made by the student concerned is correct to the best of my knowledge and belief.

**Date :**

---

**Dr. A. K. M. SADRUL ISLAM**  
Professor  
Department of Mechanical and Chemical Engineering  
Islamic University of Technology

Signature of head of the department :

---

**Dr. MD. ABDUR RAZZAQ AKHANDA**  
Head  
Department of Mechanical and Chemical Engineering  
Islamic University of Technology

# **ACKNOWLEDGEMENT**

First of all I would like to express my heartiest gratefulness to Almighty ALLAH (Sbw) who blessed us with potential and patience, which enable us to complete this thesis successfully overcoming the obstacles in the way.

I would like to thank my supervisor, Professor **Dr. A. K. M. SADRUL ISLAM** for his guidance, enthusiasm coupled with his thoughtfulness and care for students which are truly inspiring. I am extremely grateful to have his unwavering support and valuable suggestions. The supervisor had dedicated his valuable time, even at odd hours, which had ensured completion of this project.

I also express my gratefulness to the Head of Mechanical and Chemical Engineering Department **Dr. Md. Abdur Razzaq Akhanda** and all the faculty members of the department for providing me with necessary supports. This thesis would not have been possible without the help and support of few people that I am fortunate enough to have in my life. I would like to give my sincere thanks to my senior Sayedus Salehin, Muhammad Tanveer Sharif and Sheikh Remnant Rifat for their precious guidelines.

Above all I would like to thank my family specially Mother for her enormous love and mental support and giving me the opportunity to carry out a degree by helping me morally and financially through all these years. Without her unconditional support nothing would be possible from my part.

I am highly indebted to the above-mentioned persons and without their encouragement, it would have been impossible to complete this dissertation.

Although I tried my best to complete this thesis flawlessly, I seek apology if there is any mistake found in this report.

## **ABSTRACT**

Scarcity and continuous depletion of conventional energy sources gradually making renewable energy especially solar energy as an alternative energy source. One of the simplest and most direct applications of this energy is the conversion of solar radiation into heat, which can be used in water heating systems. A commonly used solar collector is the flat-plate collector. The objective of this thesis work is to investigate the heat transfer performance of nanofluid in solar collector and due to this purpose heat transfer coefficient of nanofluid, amount of heat transfer and average Nusselt number at various volume concentrations and Reynolds number were studied. Numerical simulation of  $\text{Al}_2\text{O}_3$ /water nanofluid was carried out using ANSYS-FLUENT 14.0 CFD package. This thesis deals with the convection of water and nanofluid in flat plate solar collector under steady laminar flow condition. Simulations were conducted in the range of  $500 < \text{Re} < 2000$  for both water and nanofluid. volume concentrations of nanoparticle considered in the simulation are 0 %, 0.5 % ,1 % and 2%. Particles are assumed spherical in shape with a constant diameter of 40 nm. Two phase mixture model is adopted to simulate the convection flow. Mixture model which is a simplification of the Eulerian multiphase model has been chosen prior to solving the governing equations of continuity, momentum, and energy and empirical equations are applied to calculate the thermophysical properties of nanofluid. The governing equations are solved numerically using the finite-volume approach

Result shows that, increasing the volume concentration and Reynolds number increases the heat transfer coefficient of working fluid, Nusselt number and thermal performance. For instance, at  $\text{Re} = 2000$ , convective heat transfer coefficient of nanofluid containing 2 % Vol. of  $\text{Al}_2\text{O}_3$  was observed 156% higher than water and enhancement in thermal performance is 142%.

### **Keyword :**

[Nanofluid, Laminar, Two-phase mixture model, FLUENT, Nusselt No.]

# INDEX

---

	<b>Page No.</b>
Abstract	3
List of figure	7-8
List of table	9
Nomenclature	10-11
<b>Chapter 1. Introduction</b>	<b>12-22</b>
<hr/>	
1.1 Renewable energy and Solar energy	13
1.1.1 Solar Collector	14
1.1.2 Flat Plate Solar Collector	14
1.2 Concept of Nanofluid	15
1.2.1 Common Base Fluids and Nanoparticles	16
1.2.2 Method Of Nanoparticles Production	18
1.2.3 Preparation Of Nanofluid From Nanoparticles	18
1.2.4 Nanofluid In Solar Collector	19
1.3 CFD	20
1.3.1 Two phase modeling	20
1.3.1.1 Euler-Lagrange approach	20
1.3.1.2 Euler-Euler approach	21
<b>Chapter 2. Literature Review</b>	<b>23-31</b>
<hr/>	
2.1 : Previous works based on experimental Study of Nanofluid	

2.1.1 Prashant	24
2.1.2 L. Syam <i>et al.</i>	25
2.1.3 Shung <i>et al.</i>	25
2.2 : Previous works based on Numerical Study of Nanofluid	
2.2.1 Mohammd <i>et al.</i>	26
2.2.2 Barzin <i>et al.</i>	26
2.2.3 Heyhat <i>et al.</i>	26
2.2.4 Bianco <i>et al.</i>	27
2.2.5 Kalteh <i>et al.</i>	27
2.2.6 Labib <i>et al.</i>	28
2.2.7 Demir <i>et al.</i>	29
<b>Chapter 3. Objective</b>	<b>30</b>
<hr/>	
<b>Chapter 4. Methodology</b>	<b>31-48</b>
<hr/>	
4.1 Computational Domain and Mesh	32
4.2 Governing Equations	34
4.3 Boundary Condition	37
4.4 Numerical Method	40
<b>Chapter 5. Calculation and Result</b>	<b>46</b>
<hr/>	
<b>Chapter 6. Conclusion and Future work</b>	<b>65</b>
<hr/>	
<b>References</b>	<b>67</b>
<hr/>	

## LIST OF FIGURE

---

	Page No.
Figure 1.1: Solar energy	13
Figure 1.2: Flat Plate Solar Collector	15
Figure 1.3: Nanoparticle	17
Figure 1.4: Nanofluid	18
Figure 1.5: Top-down and Bottom up process	19
Figure 2.1: Plot (Time vs Temp difference) of Prashant.	26
Figure 2.2: Plot (Volume concentration vs thermal resistance) of Shung <i>et al.</i>	28
Figure 2.3: Plot (average Nu vs Re) of Kalteh <i>et al.</i>	30
Figure 4.1: Schematic design of tube	34
Figure 4.2: Tetra mesh	34
Figure 4.3: Geometry of the computational domain	35
Figure 5.1: Plot temperature vs length along centerline for Re = 500	56
Figure 5.2: Plot temperature vs length along centerline for Re = 900	57
Figure 5.3: Plot temperature vs length along centerline for Re = 1300	57
Figure 5.4: Plot temperature vs length along centerline for Re = 1700	58
Figure 5.5: Plot temperature vs length along centerline for Re = 2000	58
Figure 5.6: Temperature contour at outlet for Re = 500	59
Figure 5.7: Temperature contour at outlet for Re = 900	60
Figure 5.8: Temperature contour at outlet for Re =1300	61
Figure 5.9: Temperature contour at outlet for Re = 1700	62
Figure 5.10: Temperature contour at outlet for Re =2000	63

Figure 5.11 : Plot The effect of nanoparticle concentration on average heat transfer coefficient	65
Figure 5.12 : Plot Average Nusselt number for nanofluid in different Reynolds and volume concentrations for 40 nm nanoparticle size	66



## LIST OF TABLE

---

	Page No.
Table 1 : Properties of water and Al <sub>2</sub> O <sub>3</sub> nanoparticle at 293 K	18
Table 5.2: The inlet, outlet and mean wall temperature Reynolds No. 500	47
Table 5.3: The inlet, outlet and mean wall temperature Reynolds No. 900	47
Table 5.4: The inlet, outlet and mean wall temperature Reynolds No. 1300	47
Table 5.5: The inlet, outlet and mean wall temperature Reynolds No. 1700	47
Table 5.6: The inlet, outlet and mean wall temperature Reynolds No. 2000	48
Table 5.7: Mean temperature difference	48
Table 5.8: Effective density of nanofluid	49
Table 5.9 : Specific heat of nanofluid	49
Table 5.10 : Mass flow rate	50
Table 5.11 : Total heat absorbed by the working fluid	50
Table 5.12 : Average heat transfer coefficient	51
Table 5.13 : Effective Thermal conductivity of nanofluid	51
Table 5.14: Average Nusselt number	52

## Nomenclature

---

### Symbol

$C_p$	Specific heat (J/kg K)
$D_p$	Nanoparticle diameter (nm)
$K$	Thermal conductivity (W/m K)
$Re$	Reynolds number
$Nu$	Nusselt number
$Gr$	Grashof number
$T$	Temperature (K)
$V$	Velocity ( $m\ s^{-1}$ )
$D$	Diameter of the tube (m)
$r$	Radius of tube (m)
$D_h$	Hydraulic Diameter of the tube (m)
$L$	Length of the tube (m)
$A$	cross-sectional area of tube ( $m^2$ )
$A_h$	Surface area of tube ( $A_h = 2\pi rL$ )
$Q$	Heat carried out by the fluid (W)
$q$	Heat flux, ( $W/m^2$ )
$h$	Average heat transfer coefficient
$a$	Particle's acceleration
$x$	Axial direction
$y$	Vertical direction
$u$	Axial velocity
$v$	Vertical velocity

### Greek letters

$\Phi$	Volume fraction
$\mu$	Dynamic viscosity ( $\text{N s m}^2$ )
$\rho$	Density ( $\text{kg m}^{-3}$ )
$\Delta$	Difference

### Subscripts

i	Inlet
o	Outlet
w	Wall
f	Base fluid
b	Bulk
p	Particle
eff	Effective

## INTRODUCTION

### Features :

#### 1.1 Renewable Energy and Solar energy

##### 1.1.1 Solar Collector

##### 1.1.2 Flat Plate Solar Collector

#### 1.2 Concept of Nanofluid

##### 1.2.1 Common Base Fluids and Nanoparticles

##### 1.2.2 Method of Nanoparticles Production

##### 1.2.3 Preparation of Nanofluids From Nanoparticles

##### 1.2.4 Nanofluid In Solar Collector

## 1.1 Renewable energy and Solar energy

Renewable energy is generally defined as energy that comes from resources which are continually replenished continuously. About 16% of global final energy consumption comes from renewable resources. Mainstream renewable technologies are Wind power, Hydropower, Tidal, Solar energy, Biomass, Biofuel and Geothermal energy. Fossil fuels are non-renewable, that is, they draw on finite resources that will eventually dwindle, becoming too expensive or too environmentally damaging to retrieve. In contrast, many types of renewable energy resources will never run out and also causes less environmental pollution.

Limited availability of fossil resources and environmental problems associated with them have emphasized the need for new sustainable energy supply options that use renewable energies. Solar energy is one of the best sources of renewable energy with minimal environmental impact. As the primary energy sources are depleting continuously, solar energy draws attention of researchers throughout the world. When dealing with solar energy, there are two basic choices. The first one is photovoltaics, which is direct energy conversion that converts solar radiation to electricity. The second is solar thermal, in which the solar radiation is used to provide heat to a thermodynamic system.

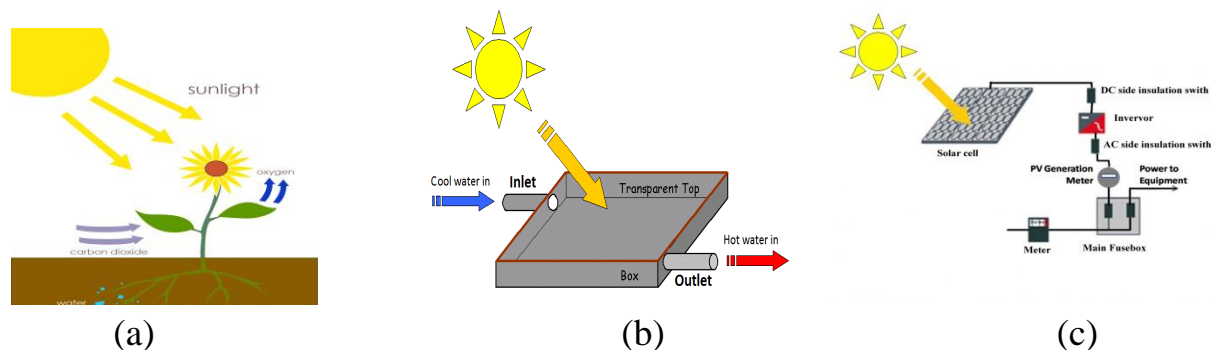


Fig. 1.1: Solar energy

### **1.1.1 Solar collector**

The conversion of solar thermal energy into more usable form is done by solar collectors. A solar collector is a device which transfers the collected solar energy to a fluid passing in contact with it, so it is always a matter of investigation to know that how efficiently solar collectors are converting solar energy into thermal energy. Solar collectors fall into two general categories [24]:

1. Concentrating Solar Collector
2. Non-concentrating Solar Collector

In the non-concentrating type, the collector area (i.e., the area that intercepts the solar radiation) is the same as the absorber area (i.e., the area absorbing the radiation). In these types the whole solar panel absorbs light. A solar collector that uses reflective surfaces to concentrate sunlight onto a small area, where it is absorbed and converted to heat. These collectors reach much higher temperatures than non-concentrating type collectors.

As the solar collectors act as a medium of converting solar energy into useful energy, it is always been a field of research to develop the efficiency of collector. Heat transfer fluids (HTFs) play an essential role in solar water heating systems by transferring collected energy from the collector, perhaps via a heat exchanger to the store. The commonly used HTF in solar collector is water, having low thermal performance which lowers the efficiency of collector.

### **1.1.2 Flat Plate Solar Collector**

Flat-plate collectors are the most commonly used non-concentrating type collector, developed by Hottel and Whillier in the 1950s, They consist of absorber, transparent cover, heat-transport fluid and heat insulating backing. Absorber is a coated metal plate that absorbs the sun's radiation and causes its temperature to rise above the ambient temperature. It covers the full aperture area of the collector and perform three functions: firstly to absorb the maximum possible amount of solar irradiance, secondly to conduct this heat into the working fluid which is circulated through a circular tube and welded to the absorber, at a minimum temperature difference and thirdly to lose a minimum amount of heat back to the surroundings.

The absorber is usually covered with one or more transparent or translucent cover sheets to reduce convective heat loss. In the absence of a cover sheet, heat is lost from the absorber as a result of not only forced convection caused by local wind but also natural convective air currents created because the absorber is hotter than ambient air.

Insulation is needed in solar thermal collectors to trap and concentrate heat energy and to improve absorption efficiency. By avoiding thermal losses through the rear and the sides of the collector, insulation enables the maximum amount of collected heat to be transferred to the circulating fluid.

The components of a Flat plate solar collectors, we are concerned about in this thesis work is the Heat transfer fluid. This fluid plays the most vital role in heat transferring.

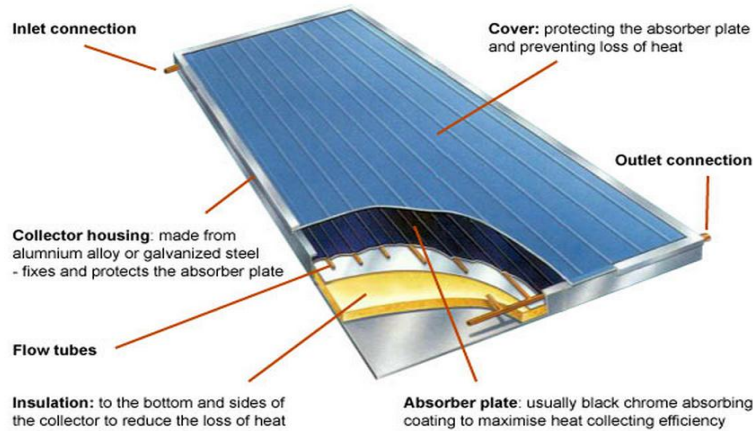


Fig. 1.2 : Flat Plate Solar Collector

## 1.2 Concept of Nanofluid :

Heat transfer is one of the most important processes in many industrial and consumer products. The inherently poor thermal conductivity of conventional fluids puts a fundamental limit on heat transfer. Therefore, for more than a century scientists and engineers have made great efforts to break this fundamental limit by dispersing millimeter- or micrometer-sized particles and later on nano-sized particles in liquids. Maxwell (1993) for the first time showed that the conductivity of liquid-solid mixtures improves with increasing particle volume fraction if solid particle[11]. As We know that thermal conductivity of solids is greater than liquids. Commonly used fluids in heat transfer applications such as water, ethylene glycol and engine oil have low thermal conductivity when compared to thermal conductivity of solids, especially metals. For example, the thermal conductivity of copper at room temperature is about 700 times greater than that of water and about 3000 times greater than that of engine oil . Therefore, the thermal conductivities of fluids that contain suspended solid metallic particles could be expected to be significantly higher than those of conventional heat transfer fluids. But we cannot add large solid particles due to certain major drawbacks. For example

- Mixtures are unstable and hence, sedimentation occurs.
- Presence of large solid particles also require large pumping power and hence cost increases.
- Solid particles may also erode the channel walls.

Well in Maxwell's study the particles were micrometer in size. Those particles caused several problems such as abrasion, clogging and pressure dropping. By improving the technology to make particles in nanometer dimensions, a new generation of solid-liquid mixtures has been generated called Nanofluid. the term 'Nanofluid'(nanoparticle fluid suspensions) was coined by Choi(1995) to describe this new class of nanotechnology-based heat transfer fluids that exhibit thermal properties superior to those of their host fluids or conventional particle fluid suspensions. Nanofluid is a new interdisciplinary field of great importance where Nanoscience, Nanotechnology and Thermal Engineering meet, has developed largely over the past decade. The goal of Nanofluids is to achieve the highest possible thermal properties at the smallest possible concentrations (preferably <1% by volume) by uniform dispersion and stable suspension of nanoparticles (usually 20-40nm) in base fluid.

### 1.2.1 Common Base Fluids and Nanoparticles

A Nanoparticle or Nanopowder is a microscopic particle with at least one dimension less than 100 nm. in simple words, nano-sized particles are called Nanoparticles. Modern fabrication technology provides great opportunities to process materials actively at nanometer scales. Nanostructured or nanophase materials are made of nanometer-sized substances engineered on the atomic or molecular scale to produce either new or enhanced physical properties not exhibited by conventional bulk solids. All physical mechanisms have a critical length scale below which the physical properties of materials are changed. Therefore, particles smaller than 100 nm exhibit properties different from those of conventional solids. The noble properties of Nanoparticles come from the relatively high surface area/volume ratio

Nanoparticles used in nanofluids have been made of various materials, such as [11]:

- |   |  |
|---|--|
| 1.Oxide ceramics ( $\text{Al}_2\text{O}_3$ , CuO) | 6. Carbon nanotubes, and                       |
| 2.Nitride ceramics( $\text{AlN}$ , SiN)           | 7. Composite materials (alloyed nanoparticles) |
| 3.Carbide ceramics (SiC, TiC)                     |  |
| 4. Metals (Cu, Ag, Au)                            |  |
| 5.Semiconductors ( $\text{TiO}_2$ , SiC)          |  |



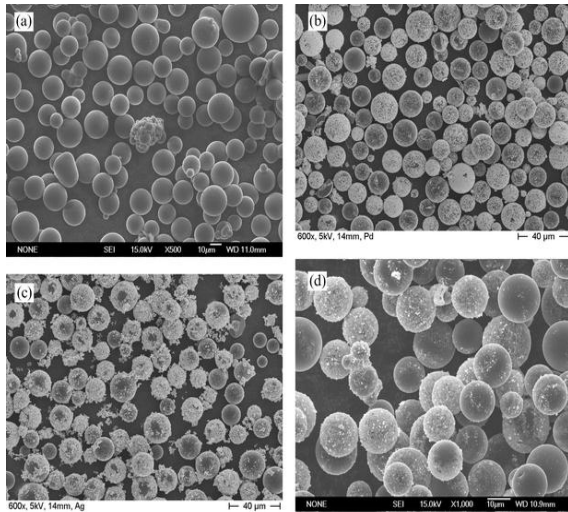


Figure 1.3 : Nanoparticle

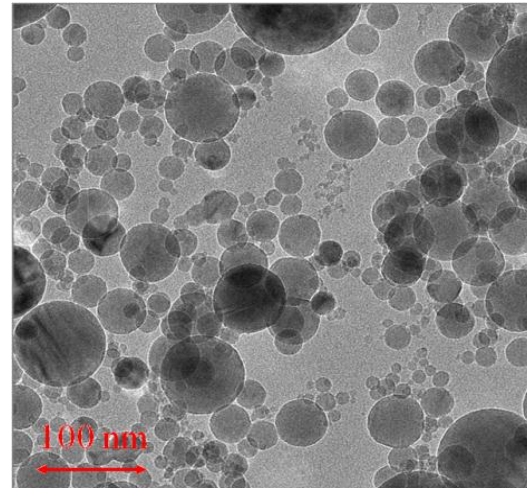


Figure 1.4 : Nanofluid

Host or Base liquid are those fluid in which nanoparticles are dispersed.

Most common fluids used to produce nanofluid are [11]:

- 1 Water
2. Ethylene Glycol (EG)
- 3.Oil

**Table 1 : Properties of water and  $Al_2O_3$  nanoparticle at 293 K**

Properties	Water	nanoparticle
Density ( $kg/m^3$ )	998.2	3900
Specific heat (J/kg.K)	4182	880
Thermal conductivity ( $W m^{-1} K^{-1}$ )	0.60	40
Molecular weight(kg/kg.mol)	18	101.92
Diameter(m)	-----	$40 \times 10^{-9}$

## 1.2.2 Method of Nanoparticles Production

Most applications require a precisely defined, narrow range of particle sizes. Specific synthesis processes are employed to produce the various nanoparticles, with desired properties for use in selected application environments.

Two basic strategies are used to produce Nanoparticles[17,18]:

1. Top-down and
2. Bottom up

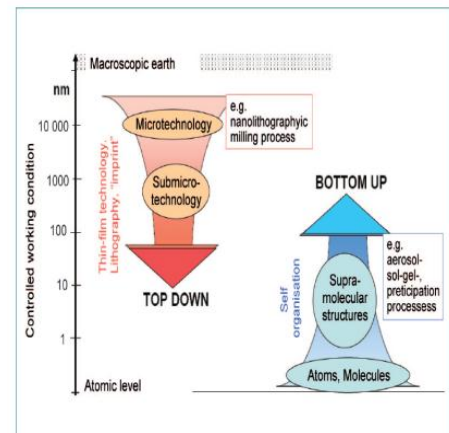


Figure 1.5 : Top-down and Bottom up process

The term “Top-down” refers here to the mechanical crushing of source material using a milling process. In the “Bottom-up” strategy, structures are built up by chemical processes via Via Pyrolysis, Inert gas, condensation, Solvothermal Reaction, Sol-gel Fabrication or Structured Media Particle size, chemical composition, crystallinity and shape can be controlled by temperature, pH-value, concentration, chemical composition, surface modifications and process control.

## 1.2.3 Preparation of Nanofluids From Nanoparticles

A very small amount of guest nanoparticles is dispersed uniformly and suspended stably in host fluids to produce nanofluids with dramatic improvements in the thermal properties of host fluids. But nanofluids are not simply liquid-solid mixtures. Some special requirements are essential e.g. even and stable suspension, durable suspension, negligible agglomeration of particles, no chemical change of the fluid, etc. In the synthesis of nanofluids, agglomeration is a major problem.

So special care should be taken at the time of synthesis.

There are mainly two techniques used to produce nanofluids[11]:

1. Single Step method
2. Two Step method

In Two Step method first nanoparticles are fabricated and then disperse nanoparticles into the base fluids where as in Single Step method making and dispersion of nanoparticle happens simultaneously. For Two Step method, dispersion techniques such as high shear and ultrasound can be used to create various particle–fluid combinations. Two step methods are most widely used for preparing Nanofluids. Most nanofluids containing oxide nanoparticles and carbon nanotubes are produced by the two-step process.

### **1.2.4 Nanofluid In Solar Collector**

The basic concept of using particles to collect solar energy was investigated by Hunt and Abdelman in 1970, who mixed the particles into gaseous fluid medium. Dispersing trace amounts of nanoparticles into common base fluids has a significant impact on thermo physical properties of base fluid. This characteristic can be used to effectively capture and transport solar radiation. Enhancement of the solar irradiance absorption capacity leads to a higher heat transfer resulting in more efficient heat transfer. Due to Brownian motion particles randomly move through liquid. And hence better transport of heat.

Benefits of use of nanofluids in solar collectors :

Nanofluids poses the following advantages as compared to conventional fluids which makes them suitable for use in solar collectors:

- Absorption of solar energy will be maximized with change of the size, shape, material and volume fraction of the nanoparticles.
- The suspended nanoparticles increase the surface area and the heat capacity of the fluid due to the very small particle size.
- The suspended nanoparticles enhance the thermal conductivity which results improvement in efficiency of heat transfer systems.
- Properties of fluid can be changed by varying concentration of nanoparticles.
- Extremely small size of nanoparticles ideally allows them to pass through pumps.
- Nanofluid can be optically selective (high absorption in the solar range and low emittance in the infrared).

## 1.3 CFD

Computational fluid dynamics, usually abbreviated as CFD, is a branch of fluid mechanics that uses numerical methods and algorithms to solve and analyze problems that involve fluid flows. Computers are used to perform the calculations required to simulate the interaction of liquids and gases with surfaces defined by boundary conditions.

In all CFD approaches the same basic procedure is followed [32]:

- During preprocessing
  - The geometry (physical bounds) of the problem is defined.
  - The volume occupied by the fluid is divided into discrete cells (the mesh). The mesh may be uniform or non-uniform.
  - The physical modeling is defined – for example, the equations of motion + enthalpy + radiation + species conservation
  - Boundary conditions are defined. This involves specifying the fluid behaviour and properties at the boundaries of the problem. For transient problems, the initial conditions are also defined.
- The simulation is started and the equations are solved iteratively as a steady-state or transient.
- Finally a postprocessor is used for the analysis and visualization of the resulting solution

### 1.3.1 Two Phase Modeling

A large number of flows encountered in nature and technology are a mixture of phases. Physical phases of matter are gas, liquid, and solid, but the concept of phase in a multiphase flow system is applied in a broader sense. In multiphase flow, a phase can be defined as an identifiable class of material that has a particular inertial response to and interaction with the flow and the potential field in which it is immersed. Currently there are two approaches for the numerical calculation of multiphase flows: the Euler-Lagrange approach and the Euler-Euler approach.

#### 1.3.1.1 Euler-Lagrange Approach

The Lagrangian discrete phase model in ANSYS FLUENT follows the Euler-Lagrange approach. The fluid phase is treated as a continuum by solving the Navier-Stokes equations, while the dispersed phase is solved by tracking a large number of particles, bubbles, or droplets through the calculated flow field. The dispersed phase can exchange momentum, mass, and energy with the fluid phase.

### 1.3.1.2 Euler-Euler Approach

In the Euler-Euler approach, the different phases are treated mathematically as interpenetrating continua. Since the volume of a phase cannot be occupied by the other phases, the concept of phase volume fraction is introduced. These volume fractions are assumed to be continuous functions of space and time and their sum is equal to one. In ANSYS FLUENT, three different Euler-Euler multiphase models are available: the volume of fluid (VOF) model, the mixture model, and the Eulerian model. The VOF model is a surface-tracking technique applied to a fixed Eulerian mesh. It is used for two or more immiscible fluids where the position of the interface between the fluids is of interest. In the VOF model, a single set of momentum equations is shared by the fluids, and the volume fraction of each of the fluids in each computational cell is tracked throughout the domain. The mixture model is designed for two or more phases (fluid or particulate). As in the Eulerian model, the phases are treated as interpenetrating continua. The mixture model solves for the mixture momentum equation and prescribes relative velocities to describe the dispersed phases.

#### Volume of Fluid (VOF) Model

The VOF formulation in ANSYS FLUENT is generally used to compute a time-dependent solution, but for problems in which concerned are only with a steady-state solution; it is possible to perform a steady-state calculation.

#### Mixture Model

The mixture model is a simplified multiphase model that can be used in different ways. The mixture model allows us to select granular phases and calculates all properties of the granular phases. This is applicable for liquid-solid flows.

The mixture model, like the VOF model, uses a *single-fluid* approach. It differs from the VOF model in two respects:

- The mixture model allows the phases to be interpenetrating. The volume fractions  $\alpha_q$  and  $\alpha_p$  for a control volume can therefore be equal to any value between 0 and 1, depending on the space occupied by phase  $q$  and phase  $p$ .
- The mixture model allows the phases to move at different velocities, using the concept of slip velocities. (Note that the phases can also be assumed to move at the same velocity, and the mixture model is then reduced to a homogeneous multiphase model.)

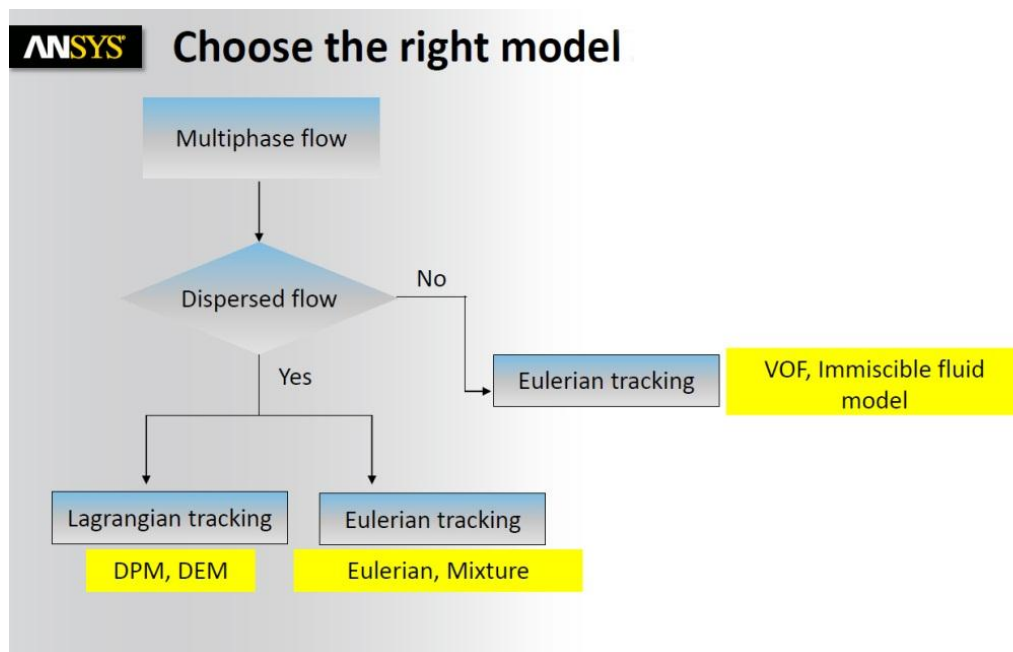
The mixture model solves the continuity equation for the mixture, the momentum equation for the mixture, the energy equation for the mixture, and the volume fraction equation for the

secondary phases, as well as algebraic expressions for the relative velocities (if the phases are moving at different velocities).

Typical Applications :

- Hydrocyclones, Bubble column reactors, suspensions, Gas sparging

In nanofluid, the nanoparticles are dispersed in base fluid. Choosing the right model for simulating nanofluid in FLUENT can be described easily by the following flow chart [25] :



## Literature Review

### Features :

#### 2.1 Previous works based on experimental Study of Nanofluid

2.1.1 Prashant *et al.*

2.1.2 L. Syam *et al*

2.1.3 Shung *et al.*

#### 2.2 Previous works based on Numerical Study of Nanofluid

2.2.1 Mohammd *et al.*

2.2.2 Barzin *et al.*

2.2.3 Heyhat *et al.*

2.2.4 Bianco *et al.*

2.2.5 Kalteh *et al.*

2.2.6 Labib *et al.*

2.2.7 Demir *et al.*

### 2.1.1 Prashant *et al.* [1]

Prashant sharma experimentally observed the thermal performance of a Direct Absorption Solar Collector( DASC) using CuO- H<sub>2</sub>O based nanofluid. DASC is more efficient collector then the conventional type solar collector, as in DASC the fluid absorbs solar thermal energy volumetrically and thus captures more heat Energy. CuO nanoparticles are synthesized by precipitation method. In their research work XRD analysis is done for the authentication of nanoparticles. Different equations were employed to determine the thermal conductivity, specific heat and viscosity of nanofluid. In their experiment they varied the volume concentration of nanoparticles and the flow rate they observed the fluid and measured the temperature difference between inlet and outlet at different times of the day. Result shows that, temperature difference increases by increasing the concentration. But at higher volume concentration the problem of settle down of nanoparticles increases, which results in lowering the collector efficiency. Optimal concentration can increase the can solar collector efficiency up to 10 – 15 %.

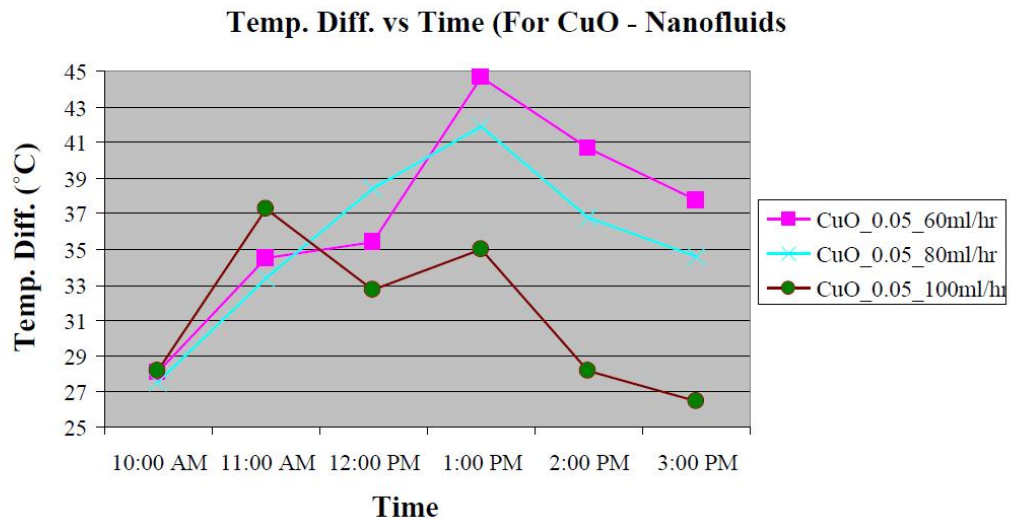


Fig. 2.1 : Time vs Temperature difference curve



### 2.1.2 L. Syam *et al.* [2]

laminar convective heat transfer and friction factor characteristics of different volume concentrations of Al<sub>2</sub>O<sub>3</sub> nanofluid in a circular tube and tube fitted with different twist ratios was investigated experimentally. In their experiment, working fluid flows through a copper tube of 0.012 m dia, from a storage tank to chiller or collecting tank, with the aid of a pump. Nusselt number of water and nanofluid of different volume fraction with increasing Reynold's number in both plain tube and tube with twisted tape inserts was calculated. Result shows that heat transfer coefficient of tube with twisted tape inserts is 29.50% greater compared to the same fluid (nanofluid with 0.5% volume concentration) and 89.76% greater than water flowing in a plain tube with Reynold's number 700. The friction factor of Al<sub>2</sub>O<sub>3</sub> nanofluid (0.5% volume concentration) with twisted tape insert is 1.0652 times greater compared to water at a 2200 Reynolds number. So at higher Reynolds numbers, use of nanofluid enhances the heat transfer coefficient with no significant enhancement in pressure drop compared to water in the range.

### 2.1.3 Shung *et al.* [3]

The nanofluid used in this study is an aqueous solution of 35 nm diameter silver nano-particles of 1 mg/l to 100 mg/l for cooling purpose. Nano-particles were first produced using a catalytic chemical vapor deposition method (NANOHUBS TECHNOLOGY CO., LTD.). The coolant circulated through the cooling chamber, where heat was removed from the condenser section by forced convection. The temperature variation in the cooling fluid was maintained within 40° C, and the operating temperature was varied over a range of 40–45° C. Result shows that the wall temperature distributions of the heat pipe containing pure water were 41.06 ° C, 40.96 ° C, 40.92 ° C, 40.89 ° C, and 40.81 ° C, respectively. After adding a small amount of silver nano-particles in the pure water, the heat pipe wall temperature became lower than that of pipes filled with pure water; from 40.56 ° C to 40.37° C. The measured results also show that the thermal resistances of the heat pipe decrease as the silver nano-particle size and concentration increase.

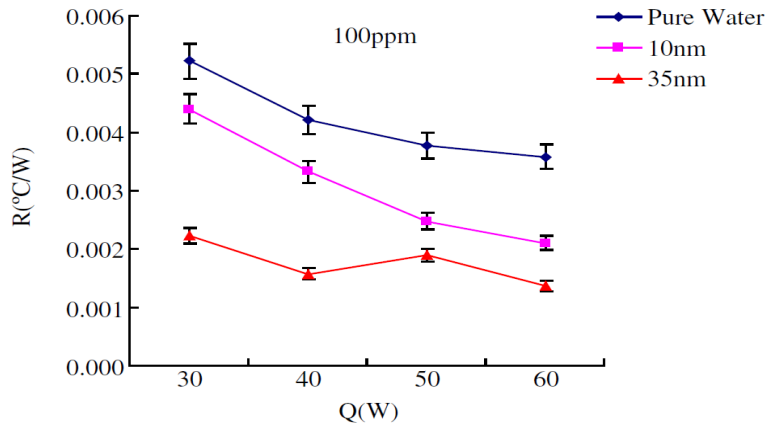


Fig. 2.2 : Volume concentration vs Thermal resistance

### 2.2.1 Mohammdd *et al.* [4]

Mohammdd et al[2] simulated the turbulent flow of Al<sub>2</sub>O<sub>3</sub>/water nanofluid in a subchannel of a typical pressurized water reactor. single-phase model was adopted to simulate the nanofluid convection of 1% and 4% by volume concentration. For the investigation they obtained the Thermophysical Properties of the Nanofluids such density, specific heat, viscosity, thermal conductivity by applying classical formulas. their results show that, the heat transfer increases with nanoparticle volume concentrations in the subchannel geometry.

### 2.2.2 Barzin *et al.* [5]

Barzin *et al* simulated the effects of both nanofluid particle size and concentration on cylindrical heat pipes thermal performance using the ANSYS-FLUENT CFD. With the increase of volume concentration, thermal resistance of a heat pipe decreases. This behaviour reverses once the concentration level reaches to a specific value and beyond. And by decreasing the particle size within the fluid, the heat pipe wall temperature distribution reduces and overall thermal conductivity of the fluid was improves. Whereas a fall in velocity magnitude was observed as the particle concentration level increases.

### 2.2.3 Heyhat *et al.* [6]

In this paper the wall shear stress and heat transfer coefficient of  $\gamma\text{Al}_2\text{O}_3$ -water nanofluids was analyzed under laminar forced convection condition in circular pipe. They assumed that the distribution of nanoparticles in the flow field is nonhomogeneous and the result show that enhancement in heat transfer is approximately 23% and 40% for the values of particle volume concentration 0.03 and 0.05 , respectively.

#### **2.2.4 Bianco *et al.* [7]**

Turbulent forced convection flow of a water- $\text{Al}_2\text{O}_3$  nanofluid in a circular tube subjected to a constant and uniform temperature at the wall is numerically analyzed. They adopted the mixture model to simulate the nanofluid convection in a tube with length of 1.0m and circular section with 0.01 m diameter. The Thermophysical Properties of the Nanofluids were calculated using different correlation . Investigations were carried out for concentration  $\phi = 0\%$ , 1%, 4%, and 6% and an imposed 350 K uniform wall temperature. The results showed that heat transfer increased according to the particles volume concentration, but it was accompanied by increasing wall-shear stress values. The highest heat transfer rates were detected, for each concentration, in correspondence to the highest Reynolds number; moreover a good agreement is found among the results of this study and the experimental correlation proposed by Pack and Cho [15].

#### **1.2.5 Kalteh *et al.* [8]**

In this paper, laminar forced convection heat transfer and Pressure drop of copper water nanofluid inside an isothermally heated microchannel is studied numerically. An Eulerian–Eulerian two-fluid model is considered to simulate the nanofluid flow inside the microchannel. The advantage of this method in comparison to homogenous modeling is that there is no need for effective thermophysical models for the nanofluid Both phases enter the channel at the inlet with the same uniform axial velocity which is specified according to the flow Reynolds number. At the channel outlet, outflow velocity boundary condition is assumed for both phases. For thermal boundary conditions, it is assumed that the nanofluid enters the channel with 293 K and the isothermal walls have a temperature of 303 K. Result shows that the pressure drop for nanofluids is slightly higher than the pressure drop for the pure water flow, while the average Nusselt number increases with increase in the Reynolds number and particle volume concentration.

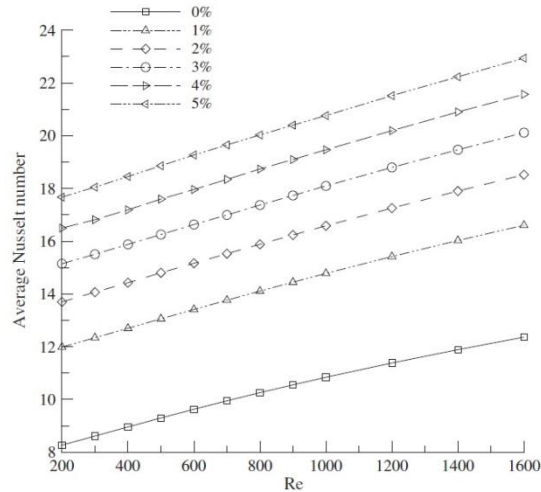


Fig. 2.3 : Average Nusselt number versus Reynolds number for different nanoparticle volume concentrations

### 1.2.6 Labib *et al.* [9]

In their study, Two different base fluids(water & ethylene glycol) are individually employed to investigate hydrodynamic and thermal behavior of base fluids on convective heat transfer mixing  $Al_2O_3$  nanoparticles. Two-phase mixture model has been chosen to study the hybrid fluid. They considered the flow as laminar flow inside a circular tube under constant heat flux at wall. Friction factor between primary phase and secondary phase was calculated from Schiller and Nauman [] FLUENT was employed to solve the problem and This set of non-linear differential equations was solved by finite volume method. The results show that Ethylene Glycol base fluid gives better heat transfer enhancement than that of water. On the other hand it was observe that wall and fluid bulk temperature decrease appreciably with the augmentation of particle loading. These results have indicate that, with the presence of such particles, the thermal properties of the resulting mixture have become considerably improved.

### 1.2.7 Demir *et al.* [10]

In this study, forced convection flows of nanofluids consisting of water with  $\text{TiO}_2$  and  $\text{Al}_2\text{O}_3$  nanoparticles in a horizontal tube with constant wall temperature are investigated numerically. Single phase model has been considered. GAMBIT was used to plot and mesh the computational geometry and the problem was solved by means of the processes in Fluent CFD program. Boundary conditions defined as velocity inlet at the pipe inlet and pressure outlet for the pipe exit. Semi Implicit Method for Pressure Linked Equations (SIMPLE) was used to pair the pressure and velocity. Results were plotted in terms of shear stress and Nusselt number for different Reynolds number at varying volume concentration. It is observed that wall shear stress increases with the increasing Reynolds number of the flow and also volume concentration of the nanoparticles in the tube as the mixture viscosity is increased strongly due to inclusion of nanoparticles and Nusselt number also increases due to the increase of heat transfer coefficient of various nanofluid volume concentrations over the base fluid for a fixed heat flux.

## **OBJECTIVE**

The thermal performance of a flat plate solar collector greatly depends on the properties of working fluid which is used to absorb the heat from solar radiation. So it has been found that the thermal properties (thermal conductivity, heat capacity, viscosity, etc.) of the fluid that is used to absorb the energy plays an important role to make the system more effective. It has been seen that conventional fluids such as water which is most commonly used, can absorb heat up to a certain limit. Which, in turn limits the efficiency of solar collector. It is expected that using nanoparticles in base fluid will enhance the thermal performance of working fluid. Thus the performance of the solar collector will improve. So this thesis is mainly focused on performance evaluation of solar collectors using nanofluids.

The main objectives of this Experimental work are as follows:

1. To investigate the temperature variation with the variation of volume fraction of nanoparticles.
2. To observe the heat transfer coefficient at different volume fraction and Reynolds number .
3. To determine the Nusselt number at different volume fraction and Reynolds number .
4. To learn ANSYS CFD and FLUENT software.
5. To compare the performance of solar collector for nanofluid and water.

# **METHODOLOGY**

## **Features :**

- 4.1 Computational Domain and Mesh
- 4.2 Governing equations
- 4.3 Boundary condition
- 4.4 Numerical method

## 4.1 : Computational Domain and Mesh

In a flat plate solar collector, working fluid flows through the circular tube which is attached to the absorber plate. For the simplicity of calculation we are considering a circular section of the tube and only fluid zone as the metal is used for tube is same for all conditions. Laminar convection of a nanofluid consisting of water and  $\text{Al}_2\text{O}_3$  nanoparticles ( $d_p = 40 \text{ nm}$ ) in a long tube with uniform heat flux around tube wall is considered. It is further assumed that the alumina-water nanofluid flow enters the channel with uniform velocity ( $V_o$ ) and temperature ( $T_o$ ) and It exchanges heat with the wall.

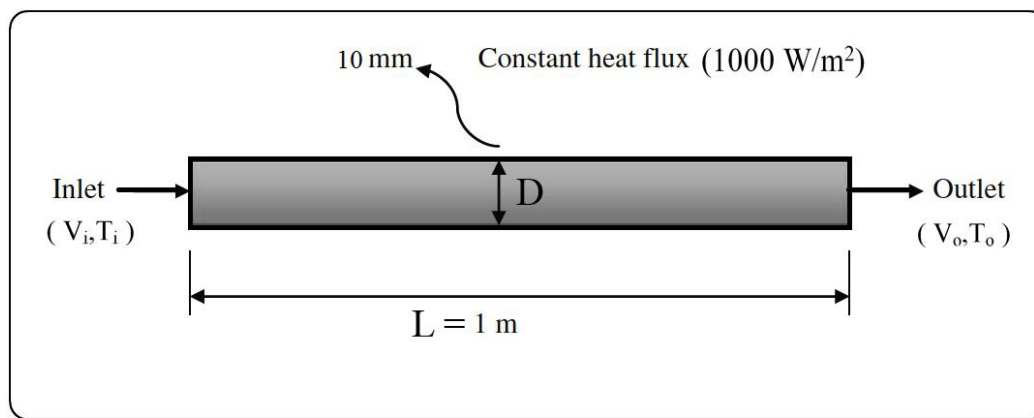


Figure 4.1 : Schematic design of tube

The volume occupied by the fluid is divided into discrete cells, which are commonly named as mesh. Tetrahedral mesh was Created on the computational domain with ANSYS ICEM 14.0. This mesh is commonly known as Tetra mesh. It is composed of four triangular faces, three of which meet at each corner or vertex. It has six edges and four vertices. Figure 4.2 shows shape and geometry of a Tetra mesh.



Fig. 4.2 : Tetra mesh



computational domain used in the numerical simulations In the present study is shown in figure 4.3 . The model geometry and mesh was generated ICEM CFD 14.0 , the preprocessing module for FLURNT software. Figure 4.3 represents three dimensional geometry of tube with uniform mesh. The length of the fluid domain is 1m and diameter is 0.01 m.

The accuracy if the final volume method depends on the quality of the mesh. Tetra meshes which are known to provide good accuracy for simple geometry and hence reduce the computational effort of CFD. For higher accuracy of the simulation result , mesh size was confined to minimum possible size. In this study mesh size was 0.001m. The quality of elements were smoothed globally upto the value 0.98. In the mesh repair option the surface meshes were smoothed. Details information of the mesh in given below

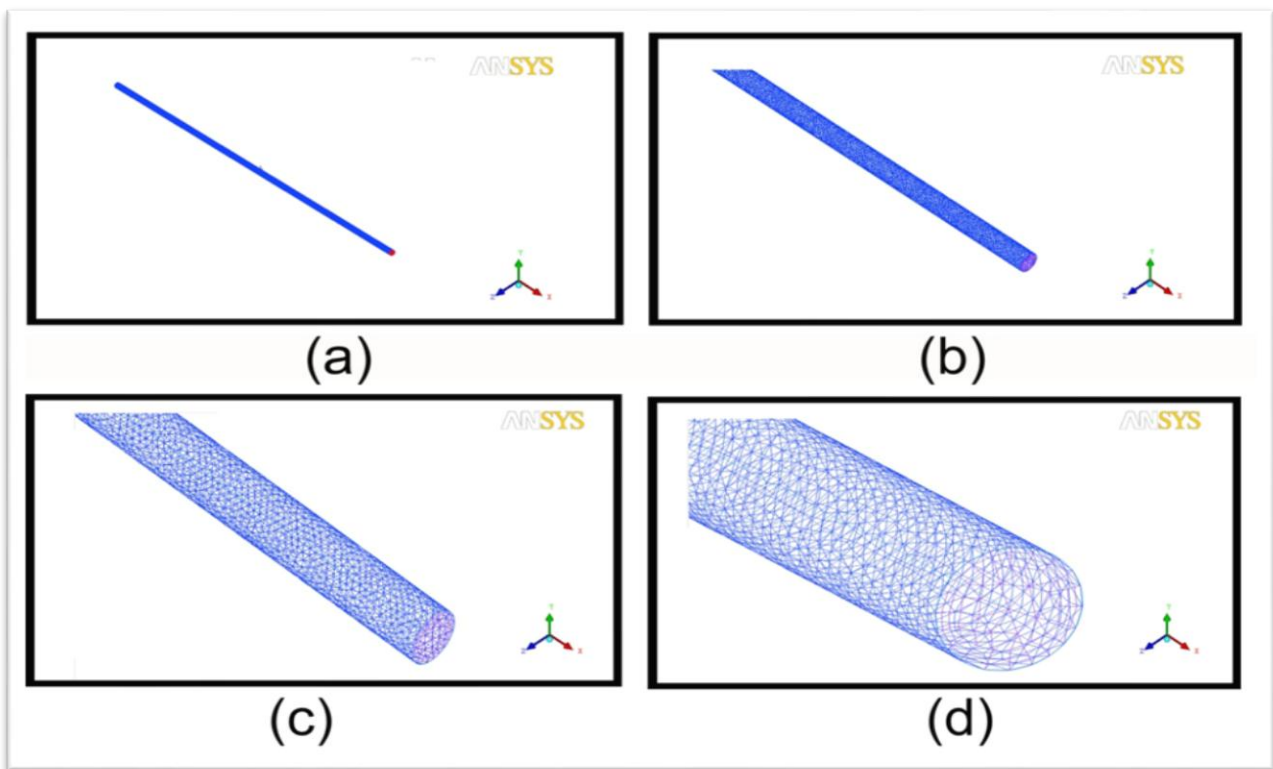


Figure 4.3 : Geometry of the computational domain and mesh

Element types :

NODE : 5  
 LINE\_2 : 803  
 TETRA\_4 : 117452  
 TRI\_3 : 37124

Element parts :

BODY : 228554  
 GEOM : 808  
 IN : 108  
 OUT : 102

PENTA\_6 : 111102  
QUAD\_4 : 120

WALL : 37034

Total elements : 266606

Total nodes : 85118

The inlet, outlet and wall zones were also created in ICEM for describing the boundary condition in FLUENT.

## 4.2 Governing Equations

Basically there are two approaches to simulate nanofluids convection, the first approach consists of the single-phase model where the fluid with the suspended nanoparticles is assumed to be continuous. Most of studies have been done using single phase (homogeneous) modeling .while the second approach uses a two-phase model in order to get a better description of the mixture taking into account the interactions between the liquid and the nanoparticles [7]. In the study of Heyhat and Kowsary a good agreement is found among the results of this study and the experimental correlation proposed by Pack and Cho [15]. This allows us to confirm that the mixture model approach for the simulation of nanofluid is satisfactory. The problem is modeled as steady state, laminar and the two dimensional. Eulerian two-phase mixture model is employed to analyze the thermal and fluid dynamic behavior of the considered nanofluid. the gravitational force is considered in the present study which is in negative direction of Y-axis. One of the major issues in these simulations is found to be the evaluation of nanofluid thermophysical properties in general and viscosity and thermal conductivity in particular, because the use of classical models is questionable for nanofluids. On the other hand, too few experimental data on nanofluids are available to build new models.

The following formulation represents the mathematical description of the mixture model governing equations

### Continuity Equation [26]:

$$\frac{\partial}{\partial t}(\rho_m) + \nabla \cdot (\rho_m \vec{v}_m) = 0 \quad (1)$$

where  $\vec{v}_m$  is the mass-average velocity;

$$\vec{v}_m = \frac{\sum_{p=1}^n \Phi_p \rho_p \vec{v}_p}{\rho_m} \quad (2)$$

and  $\rho_m$  is the mixture density

$$\rho_m = \sum_{p=1}^n \Phi_p \rho_p \quad (3)$$

$\Phi_p$  is the volume fraction of phases p.

### Momentum Equation [27]:

The momentum equation for the mixture can be obtained by summing the individual momentum equations for all phases. It can be expressed as

$$\frac{\partial}{\partial t}(\rho_m \vec{v}_m) + \nabla \cdot (\rho_m \vec{v}_m \vec{v}_m) = -\nabla p + \nabla \cdot [\mu_m (\nabla \vec{v}_m + \nabla \vec{v}_m^T)] + \rho_m \vec{g} + \vec{F} + \nabla \cdot \left( \sum_{p=1}^n \phi_p \rho_p \vec{v}_{dr,p} \vec{v}_{dr,p} \right) \quad (4)$$

where n is the number of phases,  $\vec{F}$  is a body force, and  $\mu_m$  is the viscosity of the mixture:

$$\mu_m = \sum_{p=1}^n \Phi_p \mu_p \quad (5)$$

$\vec{v}_{dr,p}$  is the drift velocity for secondary phase p :

$$\vec{v}_{dr,p} = \vec{v}_p - \vec{v}_m \quad (6)$$

### Energy Equation [28]:

The energy equation for the mixture takes the following form:

$$\frac{\partial}{\partial t} \sum_{p=1}^n (\phi_p \rho_p E_p) + \nabla \cdot \sum_{p=1}^n (\phi_p \vec{v}_p (\rho_p E_p + p)) = \nabla \cdot (k_{\text{eff}} \nabla T) + S_E \quad (7)$$

where  $k_{\text{eff}}$  is the effective conductivity.

### Volume fraction equation for secondary phases [30]

From the continuity equation for secondary phase p, the volume fraction equation for secondary phase p can be obtained:

$$\nabla \cdot (\phi_p \rho_p \vec{v}_m) = -\nabla \cdot (\phi_p \rho_p \vec{v}_{\text{dr},p}) \quad (8)$$

Due to the very small size of the particles, the lift force is neglected in the present study. The function  $f_{\text{drag}}$  is taken from Schiller and Naumann

$$f_{\text{drag}} = \begin{cases} 1 + 0.15 \text{Re}_p^{0.687} & \text{Re}_p \leq 1000 \\ 0.0183 \text{Re}_p & \text{Re}_p > 1000. \end{cases} \quad (9)$$

Where  $\text{Re}_p$  is the particle Reynolds number

$$\text{Re}_p = (V_m d_p / v_{\text{eff}})$$

The relative velocity (also referred to as the slip velocity) is defined as the velocity of secondary phase or nanoparticles (p) relative to the velocity of primary phase or base fluid (f)[29]:

$$\vec{v}_{p/f} = \vec{v}_p - \vec{v}_f \quad (10)$$

The relative velocity is determined from Eq. (11) proposed by Manninen et al [13]

$$\vec{V}_{pf} = \frac{\rho_p d_p^2}{18\mu_f f_{drag}} \frac{(\rho_p - \rho_m)}{\rho_p} \vec{a}, \quad (11)$$

The acceleration in (11) is

$$\vec{a} = g - (\vec{V}_m \cdot \vec{\nabla}) V_m. \quad (12)$$

### 4.3 Boundary Condition

Nanofluid composed of water and Al<sub>2</sub>O<sub>3</sub> nanoparticles flowing in a long tube and constant heat flux of 1000 w/m<sup>2</sup> was applied around tube wall. Both phases enter at the inlet of the tube with the same uniform axial velocity which is specified according to the flow Reynolds number and a constant inlet temperature were assigned at the channel inlet. Different volume fraction (0, 0.005, 0.01 and 0.02) were specified at the inlet for different volume concentration (0 %, 0.5%, 1 % and 2% ) of the secondary phase. The direction of the flow was defined normal to the boundary. At the channel outlet, outflow velocity boundary condition is considered for both phases. Hydraulic diameter and length of the circular tube were 0.01 m and 1 m, respectively. The length of the computational domain is chosen long enough so that the flow exits the pipe with fully developed velocity.

### 4.4 Numerical Method

The computational fluid dynamic commercial code FLUENT [19] is employed to solve the present problem. The set of non-linear differential equations was solved by finite volume method. Finite volume method converts the governing equations to a set of algebraic equations that can be solved numerically. The algebraic “discretize equations”, resulting from spatial integration process, are sequentially solved throughout the physical domain considered. FLUENT solves the systems resulting from discretization schemes using a numerical method.

The basic layout of FLUENT simulation is given in the below

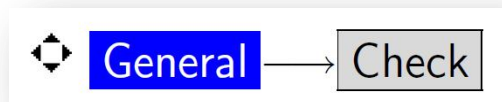
### Step 1: Mesh

The mesh created in ICEM CFD was saved in .cfx5 format for importing in FLUENT solver. Steps of importing mesh is given in the below

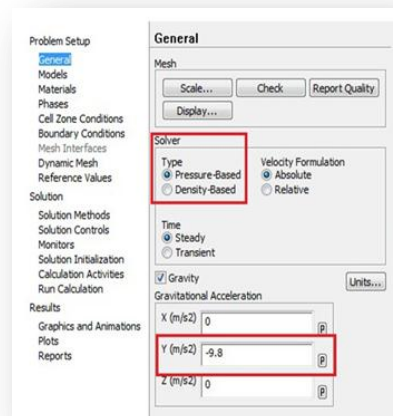


### Step 2: General Setting

After importing the mesh FLUENT will perform various check on the mesh and will report the progress in the console.

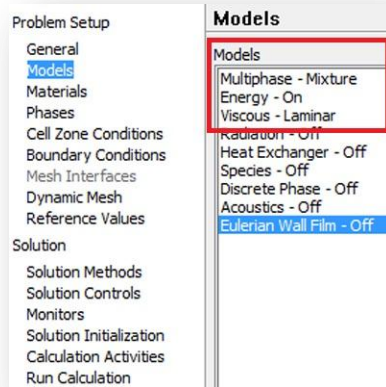


FLUENT uses two types of solver, one is pressure based and another is density based. In this thesis work pressure based solver is selected and as nanoparticles has certain weight Gravitational acceleration is considered.



### Step 3: Models

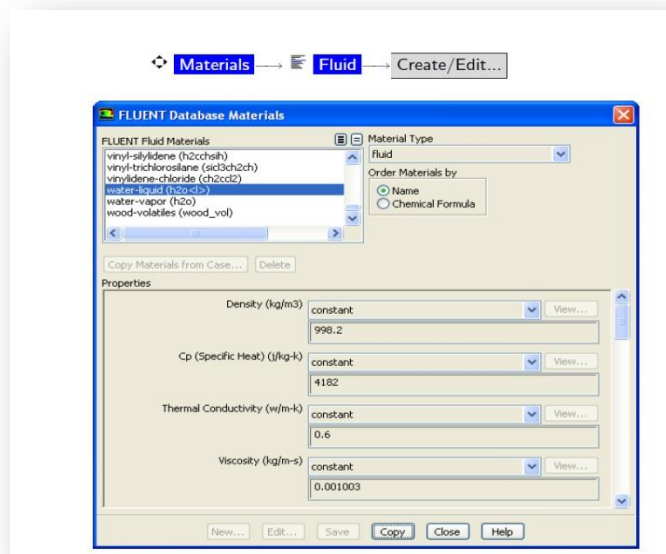
In model setting, multiphase mixture model considered. Heat flux is applied on the wall and to activate the calculation of heat transfer, the Energy Equation option was enabled in the Energy dialog box. Laminar flow was also mentioned here.



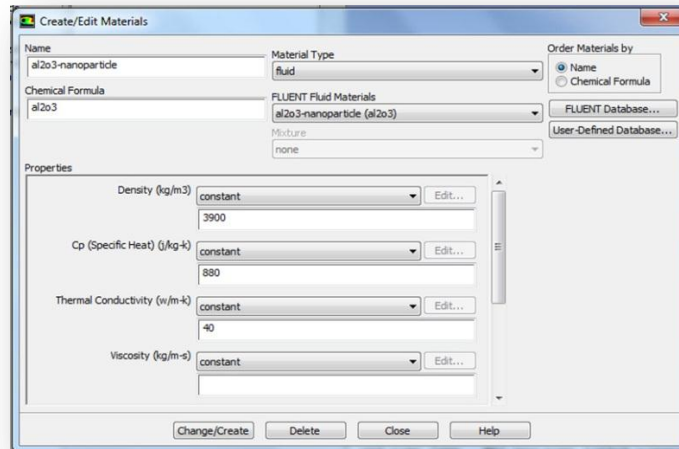
#### Step 4 : Materials

Water and nanofluid was flowed through tube and nanofluid is consist of water and  $Al_2O_3$  nanoparticles .So it is necessary to mention the thermophysical properties of water and  $Al_2O_3$  nanoparticles.

The properties for liquid water was copied from the material database so that it can be used for the primary phase.

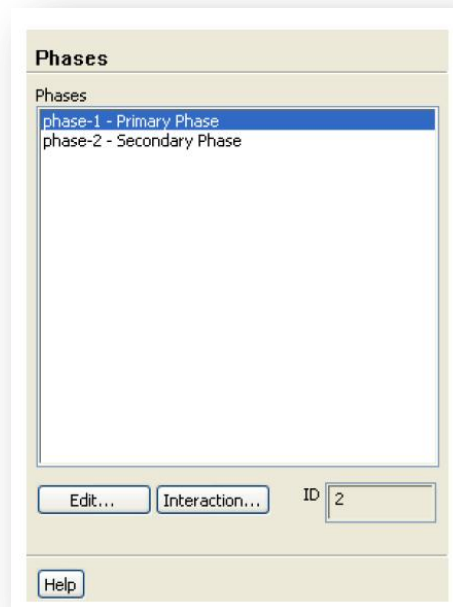


For the secondary phase the properties of  $Al_2O_3$  particles was mention which were achieved from internet and other sources.

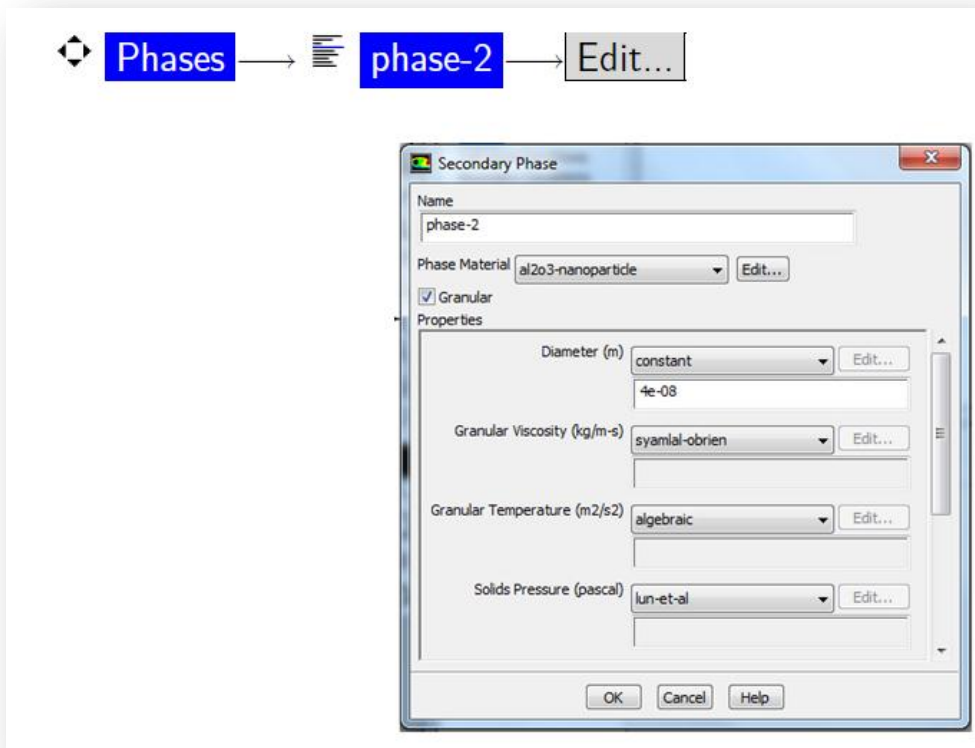
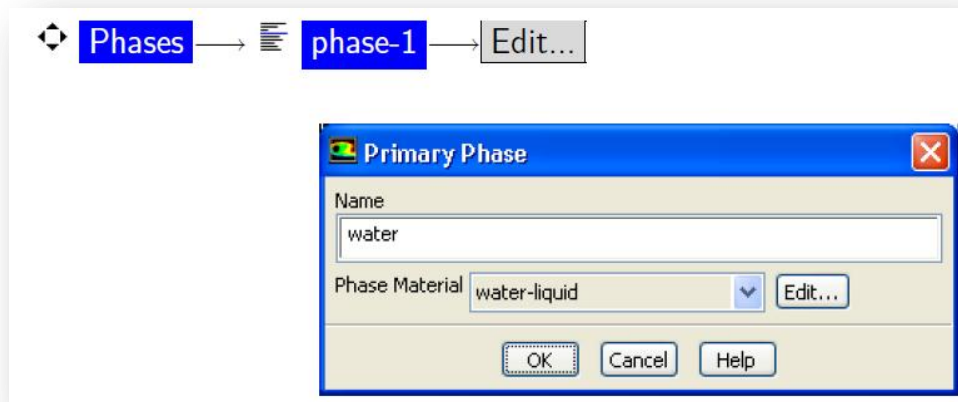


## Step 5: Phase

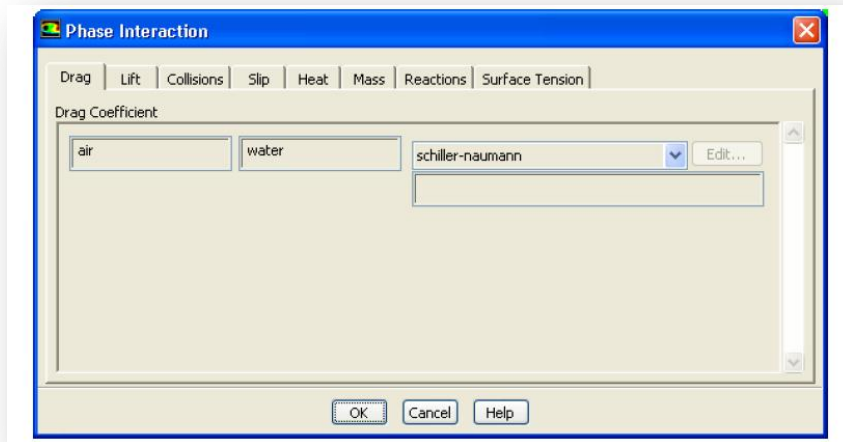
After selecting the materials, it is necessary to the phase for multiphase model. In case of nanofluid the primary phase is water and secondary phase is  $\text{Al}_2\text{O}_3$  particles. The diameter of particles was considered 40 nm in this study which was mentioned in this section.





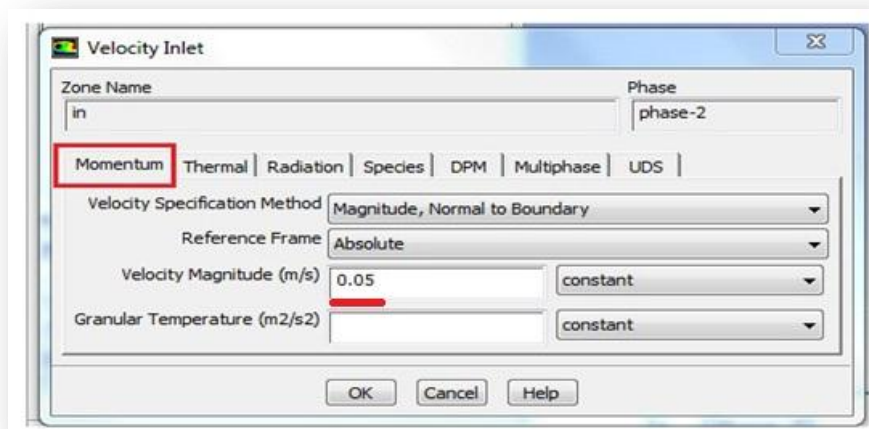
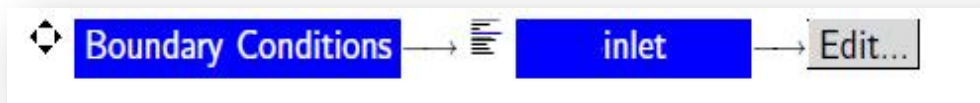


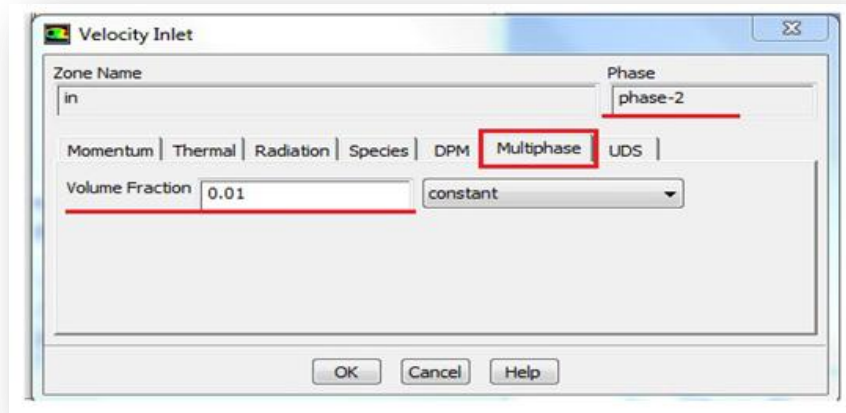
From the Drag Coefficient drop-down list schiller – naumann was selected . The Schiller-Naumann drag law describes the drag between the spherical particles and the surrounding liquid water for a wide range of conditions. In this case the nanoparticles have an approximately spherical shape with a diameter of 40 nm.



## Step 6: Boundary Conditions

Inlet boundary condition was given according to the flow Reynolds number and nanoparticles volume concentration for different conditions. For example, the velocity magnitude for  $Re = 500$  and volume concentration 1 % is shown below

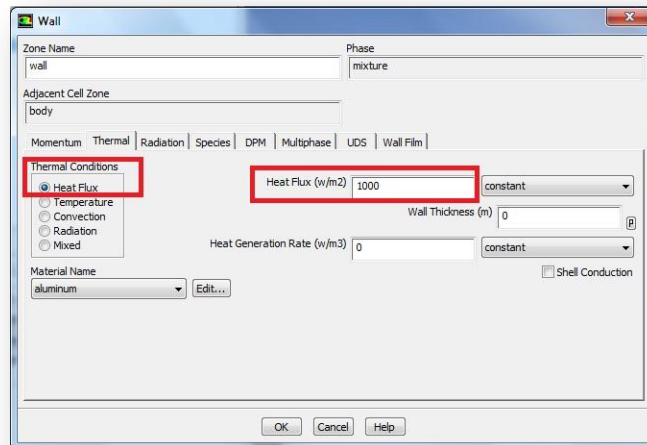




At the outlet, outflow boundary condition was applied.

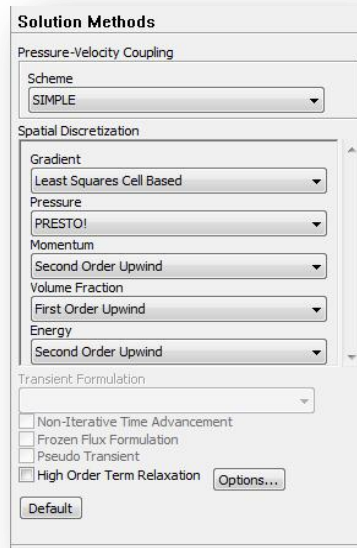


At the wall 1000 W/m<sup>2</sup> Heat flux was mentioned.

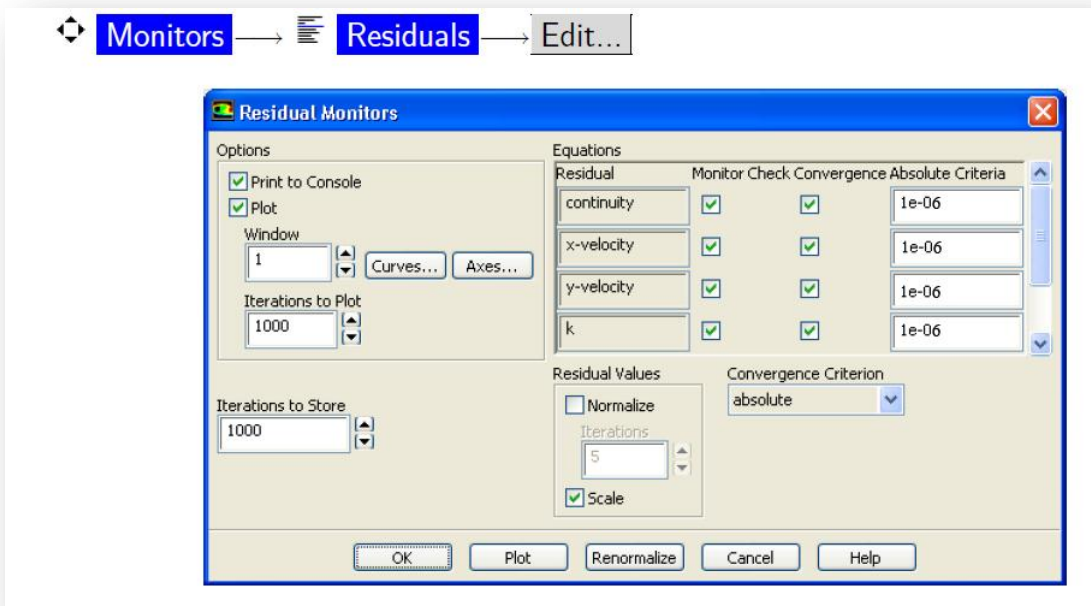


Under Relaxation Factors (URF) were set for pressure, velocity, temperature, turbulent kinetic energy and dissipation rate to 0.3, 0.7, 0.8, 0.8 and 0.8, Respectively. Semi Implicit Method for Pressure Linked Equations (SIMPLE) algorithm was used to resolve the coupling between velocity and pressure fields. The second-order upwind

scheme was used for discretization of convection energy. In case of pressure-based solver for solution method, PRESTO! Is selected as the spatial discretization method for Pressure is recommended approach

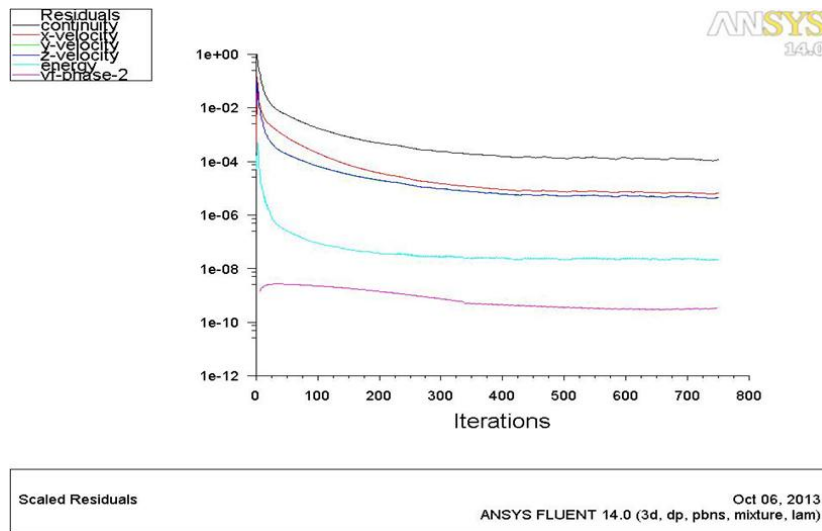
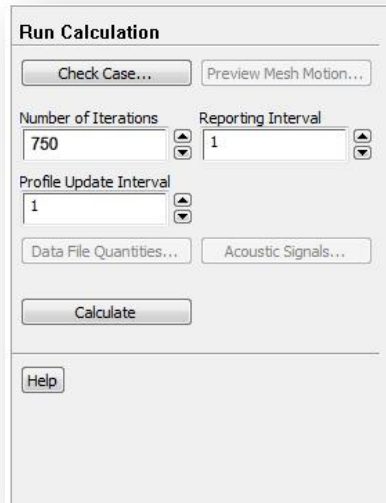


During the process, these residual were constantly monitored and scrutinized. The converged solution was keep maintained to achieve with very low level of these residual about  $10^{-6}$ .



## Step 7: Run calculation

After all the necessary setting and solution initialization the calculation was started by requesting 750 iterations. At this limit the calculation was almost converged.



After the convergence of simulation in FLUENT, the result file was exported to CFD-POST for postprocessing.

## Calculation and Result

Results are reported in terms of the average Nusselt number, average convective heat transfer coefficient and temperature along centerline as a function of Re ranging from 500 to 2000 and particle volume concentrations of 0%, 0.5%, 1%, and 2%. Results were obtained by the two-phase approach with the constant heat flux  $q = 1000 \text{ W/m}^2$  on the wall. In all cases the particles size was considered equal to 40 nm.

For calculating the average Nusselt number the following formula was used

$$\overline{Nu} = \frac{\overline{h}D_h}{k_{eff}} \quad (13)$$

The Hydraulic diameter of the tube is calculated by following formula for closed channel circular flow

$$D_h = 4 \pi R^2 / 2 \pi R = 2 R = D = 0.01\text{m}$$

The inlet, outlet and mean wall temperature obtained from CFD-POST for different Reynolds number and volume concentration are given below in tables.

Mean wall temperature was calculated from the following equation.

$$T_{wall} = \frac{1}{10} (T_{w1} + T_{w2} + T_{w3} + \dots + T_{w9} + T_{w10}) \quad (14)$$

Where  $T_{w1}, T_{w2}, T_{w3}, \dots, T_{w9}, T_{w10}$  are temperatures on the wall at 100 mm interval from the inlet boundary respectively and obtained from CFD -POST.

**Table 5.2 : Reynolds No. 500**

<b>Volume concentration(%)</b>	<b>T<sub>in</sub> (K)</b>	<b>T<sub>out</sub> (K)</b>	<b>T<sub>wall</sub> (K)</b>
<b>0</b>	300	301.396	303.034
<b>0.5</b>	300	301.479	302.62
<b>1</b>	300	301.536	302.352
<b>2</b>	300	301.616	302.02

**Table 5.3 : Reynolds No. 900**

<b>Volume concentration(%)</b>	<b>T<sub>in</sub> (K)</b>	<b>T<sub>out</sub> (K)</b>	<b>T<sub>wall</sub> (K)</b>
<b>0</b>	300	300.68	302.22
<b>0.5</b>	300	300.736	301.91
<b>1</b>	300	300.773	301.73
<b>2</b>	300	300.824	301.43

**Table 5.4 : Reynolds No.1300**

<b>Volume concentration(%)</b>	<b>T<sub>in</sub> (K)</b>	<b>T<sub>out</sub> (K)</b>	<b>T<sub>wall</sub> (K)</b>
<b>0</b>	300	300.435	301.823
<b>0.5</b>	300	300.475	301.551
<b>1</b>	300	300.503	301.386
<b>2</b>	300	300.541	300.161

**Table 5.5 : Reynolds No. 1700**

<b>Volume concentration(%)</b>	<b>T<sub>in</sub> (K)</b>	<b>T<sub>out</sub> (K)</b>	<b>T<sub>wall</sub> (K)</b>
<b>0</b>	300	300.325	301.506
<b>0.5</b>	300	300.353	301.341
<b>1</b>	300	300.374	301.189
<b>2</b>	300	300.404	300.99

**Table 5.6 : Reynolds No. 2000**

Volume concentration(%)	T <sub>in</sub> (K)	T <sub>out</sub> (K)	T <sub>wall</sub> (K)
0	300	300.285	301.405
0.5	300	300.312	301.192
1	300	300.327	301.049
2	300	300.352	300.34

The average heat transfer coefficient is used to investigate the heat transfer. It is defined by

$$\bar{h} = \frac{Q}{A_h \Delta T_m} \tag{15}$$

The mean temperature difference between the wall and the fluid is defined as

$$\Delta T_m = \frac{1}{10} (T_{w1} + T_{w2} + T_{w3} + \dots + T_{w9} + T_{w10}) - \frac{1}{2} (T_{out} + T_{in}) \tag{16}$$

Using the above equation (16) mean temperature difference for varying volume concentration at different Reynolds number are given in the table 7.

**Table 5.7: Mean temperature difference**

Volume concentration(%)	Re = 500 (K)	Re = 900 (K)	Re = 1300 (K)	Re = 1700 (K)	Re = 2000 (K)
0	2.332	1.88	1.60	1.40	1.26
0.5	1.88	1.56	1.31	1.164	1.037
1	1.584	1.34	1.12	1.002	0.886
2	1.31	1.013	0.889	0.788	0.664

In equation (15), A<sub>h</sub> is the surface area of the circular tube, calculated as

$$A_h = 2 \cdot \pi \cdot r \cdot L \tag{17}$$

Q is the total heat carried out by the flowing working fluid which can be calculated as.

$$Q = \dot{m} \cdot C_p \cdot (T_{out} - T_{in}) \tag{18}$$



Mass flow rate (  $\dot{m}$  ) is measured by  $\dot{m} = \rho_{\text{eff}} \cdot A \cdot V$  (19)

As at different Reynolds number and volume concentration of nanoparticles the velocity and density of nanofluid changes, the mass flow rate changes accordingly. So it is necessary to calculate the effective density. The effective density of the working fluid is calculated by using classical formulas developed for conventional solid-liquid mixtures

$$\rho_{\text{eff}} = (1-\phi) \rho_{\text{bf}} + \phi \rho_p \quad (20)$$

water is considered as base fluid and  $\text{Al}_2\text{O}_3$  nanoparticle as secondary phase for simulation. At 293K temperature density of base fluid ( $\rho_{\text{bf}}$ ) is  $998.2 \text{ kg/m}^3$  and density of  $\text{Al}_2\text{O}_3$  nanoparticle ( $\rho_p$ ) is  $3900 \text{ kg/m}^3$ .

Using this relation, the density of nanofluid at different volume fraction is calculated.

**Table 5.8: Effective density of nanofluid**

Volume concentration(%)	Effective density, $\rho_{\text{eff}}$ ( $\text{kg/m}^3$ )
0	998.2
0.5	1012.26
1	1026.72
2	1056.47

Again Specific heat at constant pressure ( $C_p$ ) of the fluid changes due to the change in concentration of particles. The effective Specific heat of nanofluid is obtained from correlation by Hamilton and Crosser [14].

$$C_{\text{eff}} = \{(1 - \phi_p) \rho_f c_f + \phi_p \rho_p c_p\} / \rho_{\text{eff}} \quad (21)$$

**Table 5.9: Specific heat of nanofluid**

Volume concentration(%)	Specific heat, $C_p$ (J/kg.K)
0	4182
0.5	4165
1	4148
2	4115

**Table 5.10: Mass flow rate**

Volume concentration(%)	$\dot{m}$ at Re = 500 (kg/s)	$\dot{m}$ at Re = 900 (kg/s)	$\dot{m}$ at Re = 1300 (kg/s)	$\dot{m}$ at Re = 1700 (kg/s)	$\dot{m}$ at Re = 2000 (kg/s)
0	0.00391	0.00705	0.0101	0.0130	0.0155
0.5	0.00397	0.00714	0.0103	0.0135	0.01573
1	0.0040	0.00724	0.0104	0.0137	0.0160
2	0.0042	0.00746	0.0107	0.0141	0.0165

Using equation (18), the total heat carried out by the flowing working fluid for varying volume concentration at different Reynolds number are given in the table 11.

**Table 5.11: Total heat absorbed by the fluid**

Volume concentration(%)	at Re = 500 (W)	at Re = 900 (W)	at Re = 1300 (W)	at Re = 1700 (W)	at Re = 2000 (W)
0	22.82	20.04	18.37	17.66	18.47
0.5	24.45	21.89	20.37	19.84	20.30
1	25.48	23.21	21.69	21.25	21.701
2	27.33	25.92	23.62	23.44	23.9

For water the thermal conductivity is constant at standard temperature which is  $0.60 \text{ W m}^{-1} \text{ K}^{-1}$  but adding nanoparticles change the thermal conductivity . The effective thermal conductivity of nanofluid is calculated from following Maiga *et al.* [16] formula :

$$K_{\text{eff}} = k_{\text{bf}} (4.97\Phi^2 + 2.72 \Phi + 1) \quad (22)$$

Where  $k_{\text{bf}}$  = thermal Conductivity of Base fluid =  $0.6 \text{ W m}^{-1} \text{ K}^{-1}$

**Table 5.12 : Effective Thermal conductivity**

<b>Volume concentration(%)</b>	<b>Thermal conductivity (<math>K_{eff}</math>) (<math>W m^{-1} K^{-1}</math>)</b>
<b>0</b>	0.60
<b>0.5</b>	0.605
<b>1</b>	0.616
<b>2</b>	0.633

Using equation (15), the Average heat transfer coefficient for varying volume concentration at different Reynolds number are given in the table 13.

**Table 5.13: Average heat transfer coefficient**

<b>Volume concentration(%)</b>	<b>at Re = 500 (<math>W m^{-2} K^{-1}</math>)</b>	<b>at Re = 900 (<math>W m^{-2} K^{-1}</math>)</b>	<b>at Re = 1300 (<math>W m^{-2} K^{-1}</math>)</b>	<b>at Re = 1700 (<math>W m^{-2} K^{-1}</math>)</b>	<b>at Re = 2000 (<math>W m^{-2} K^{-1}</math>)</b>
<b>0</b>	155.82	169.73	182.82	200.86	233.46
<b>0.5</b>	207.09	223.44	247.60	271.41	311.86
<b>1</b>	256.14	275.81	308.37	337.70	399.19
<b>2</b>	332.32	356.56	426.41	473.66	596.95

Using equation(13), the Average Nusselt number for varying volume concentration at different Reynolds number are given in the table 13.

**Table 5.14: Average Nusselt number**

volume concentration (%)	Nu
0	2.59
0.5	3.42
1	4.15
2	5.25

**Re = 500**

volume concentration (%)	Nu
0	2.67
0.5	3.69
1	4.47
2	5.62

**Re = 900**

volume concentration (%)	Nu
0	3.04
0.5	4.09
1	5.0
2	6.72

**Re = 1300**

volume concentration (%)	Nu
0	3.34
0.5	4.47
1	5.48
2	7.48

**Re = 1700**

volume concentration (%)	Nu
0	3.89
0.5	5.15
1	6.48
2	9.43

**Re = 2000**

## Temperature Distribution :

There is a steady increase in the fluid temperature distribution along the channel for all the cases. As the fluid moves along the channel, it absorbs heat. The bulk temperature for  $\phi = 0.5\%$  or  $\phi = 2\%$  is higher than the case of base fluid. The FLUENT results point to the temperature increase due to the presence of the particles considering the constant heat flux at the wall for all cases. It is Observed that the inclusion of nanoparticles has a beneficial effect on the wall and bulk temperatures of the nanofluid compared to base fluid.

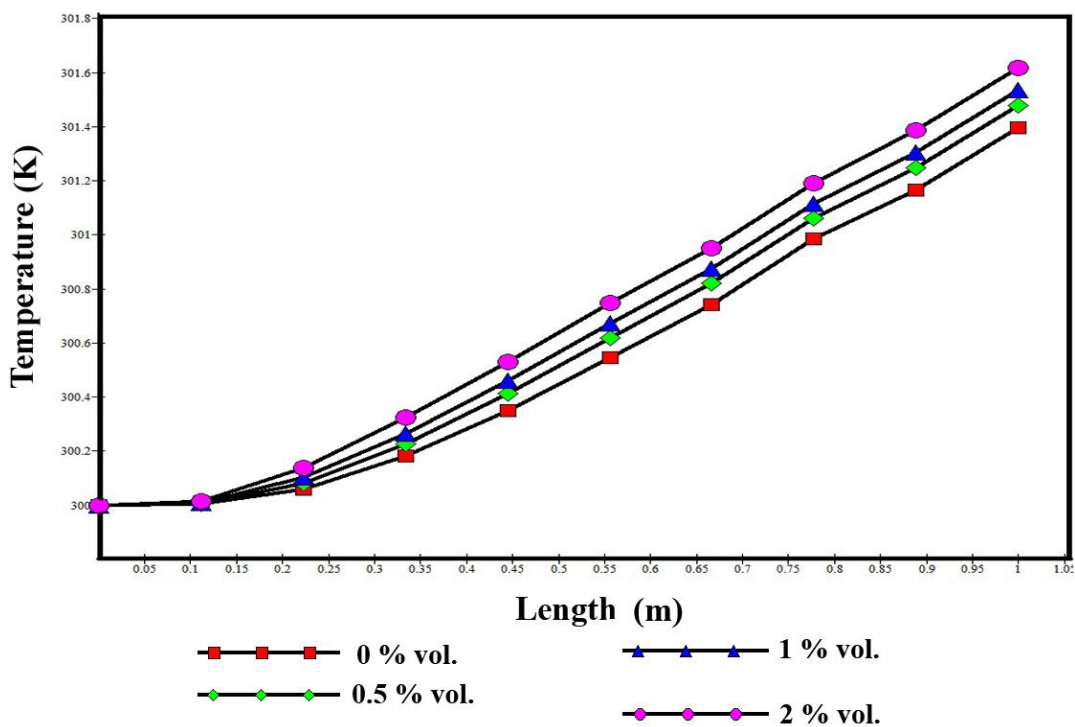


Figure 5.1: Temperature distribution along centerline of tube for different volume concentration at  $Re = 500$

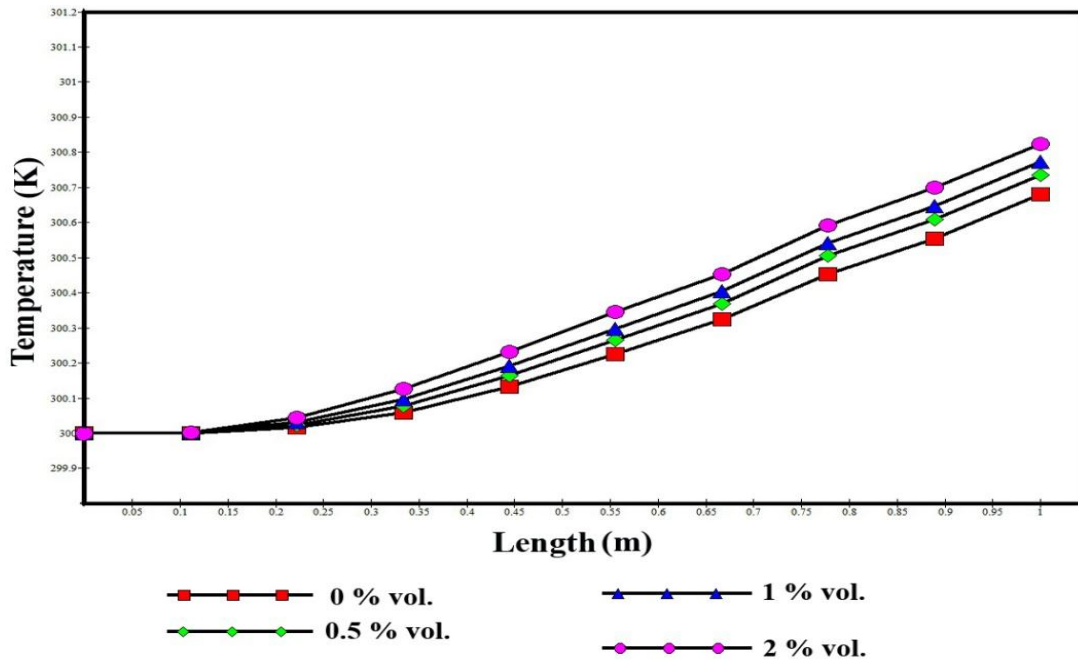


Figure 5.2: Temperature distribution along centerline of tube for different volume concentration at  $Re = 900$

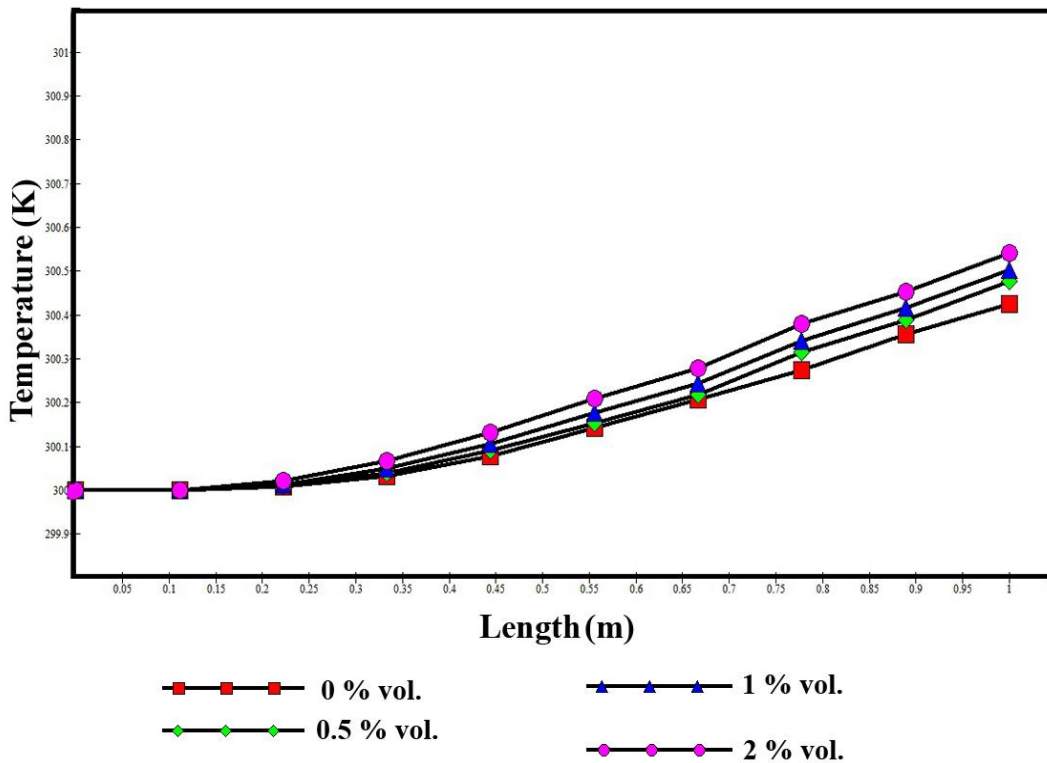


Figure 5.3: Temperature distribution along centerline of tube for different volume concentration at  $Re = 1300$

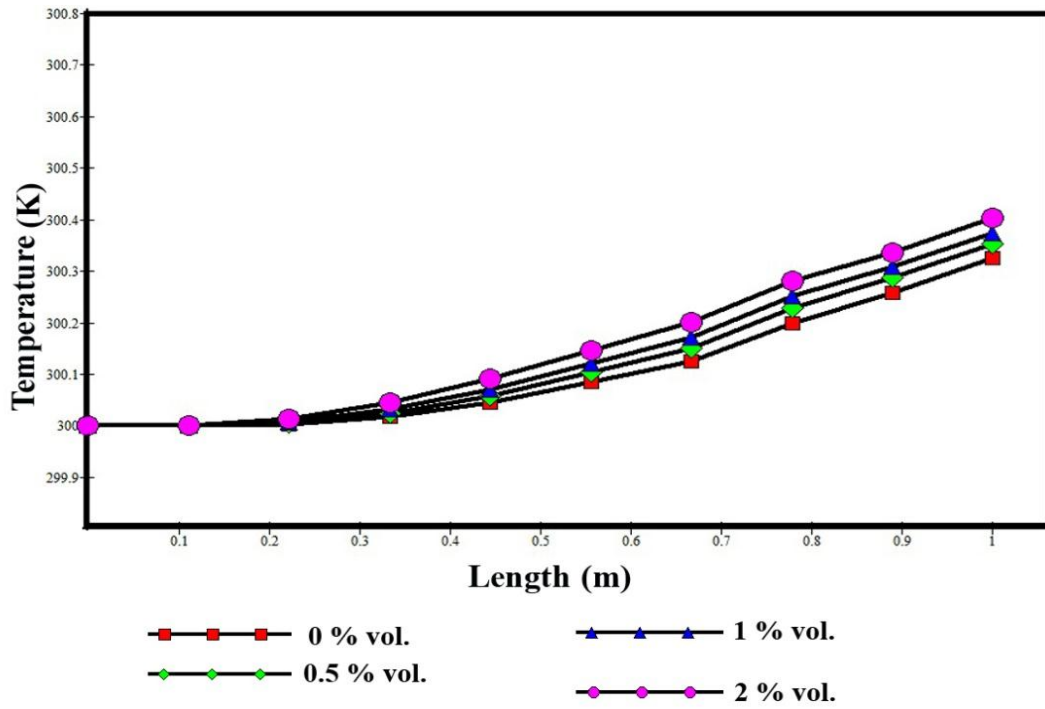


Figure 5.4: Temperature distribution along centerline of tube for different volume concentration at Re = 1700

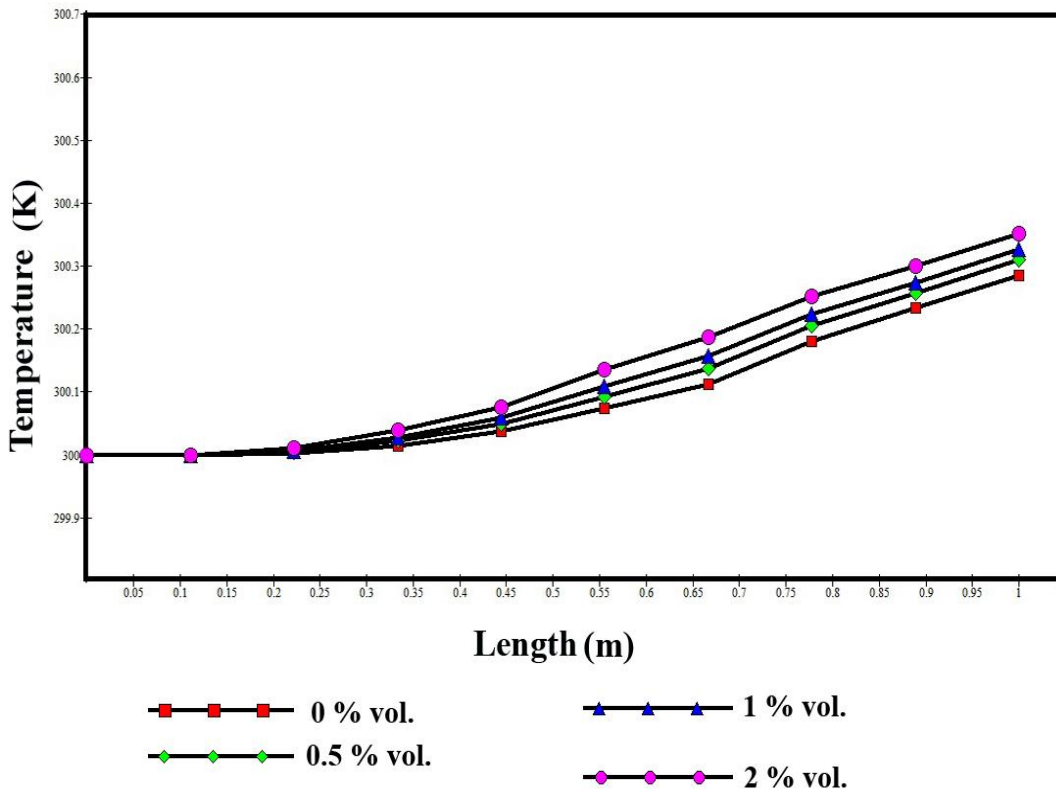


Figure 5.5: Temperature distribution along centerline of tube for different volume concentration at Re = 2000

Contours of temperature at the outlet for base fluid and nanofluids of varying concentration and at different  $Ru$  are shown in the Figures below

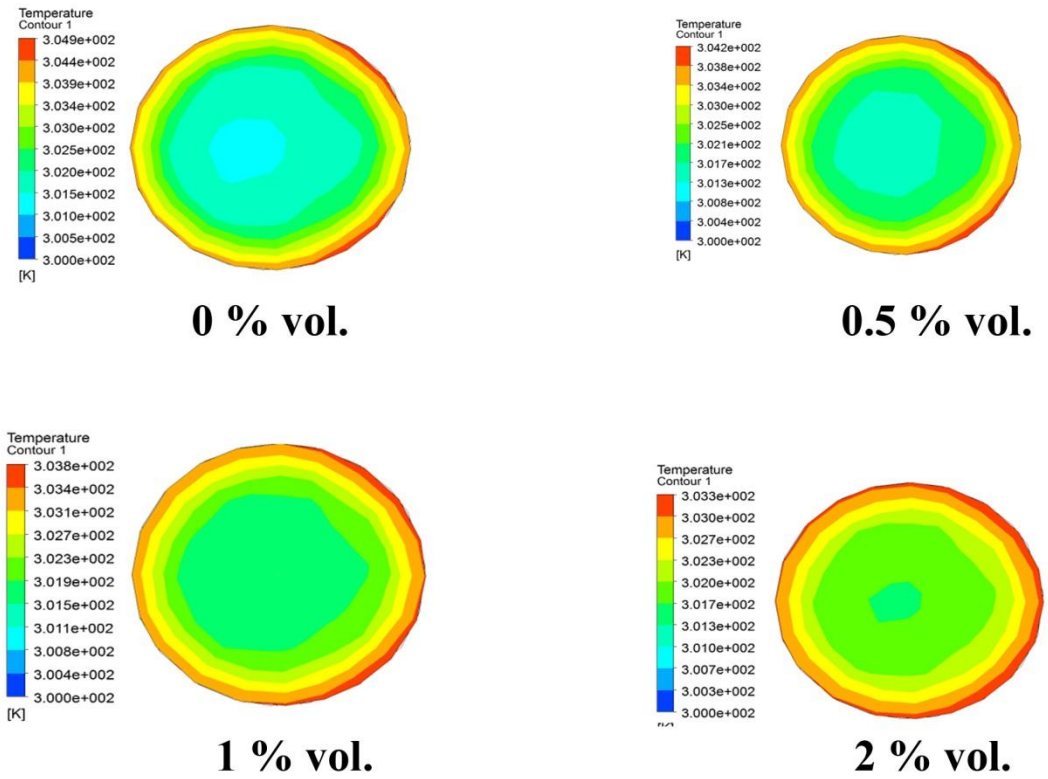


Figure 5.6: Temperature contour at outlet for  $Re = 500$



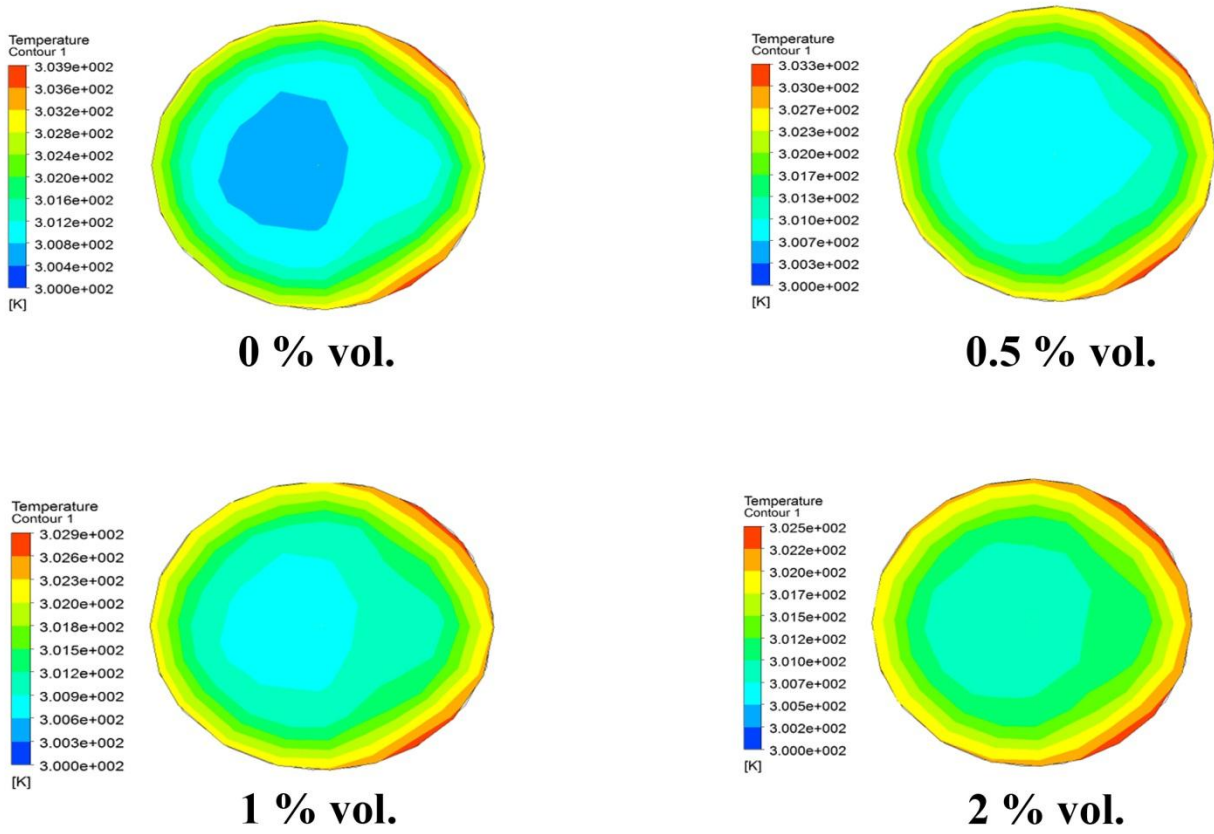
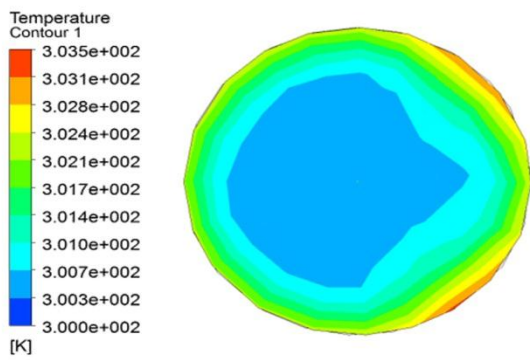
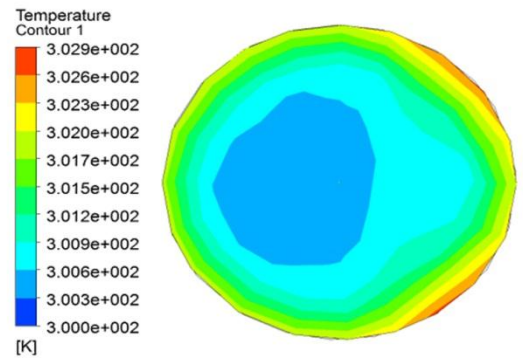


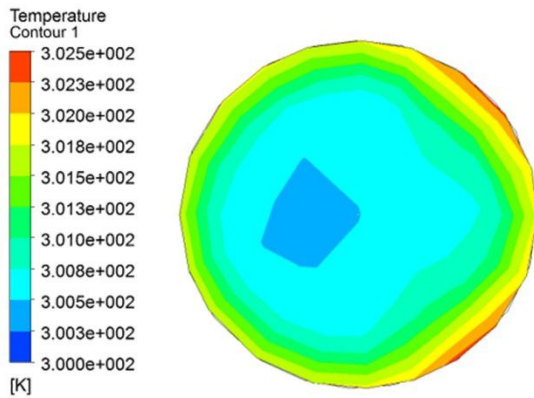
Figure 5.7: Temperature contour at outlet for  $Re = 900$



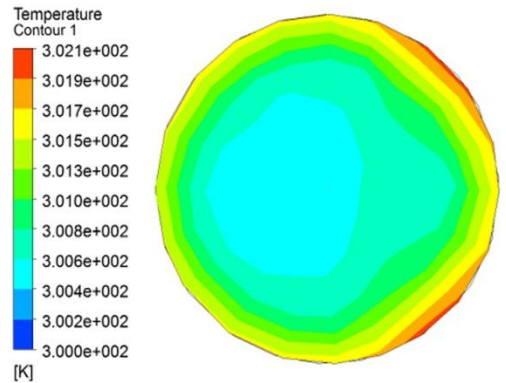
**0 % vol.**



**0.5 % vol.**



**1 % vol.**



**2 % vol.**

Figure 5.8: Temperature contour at outlet for  $Re = 1300$

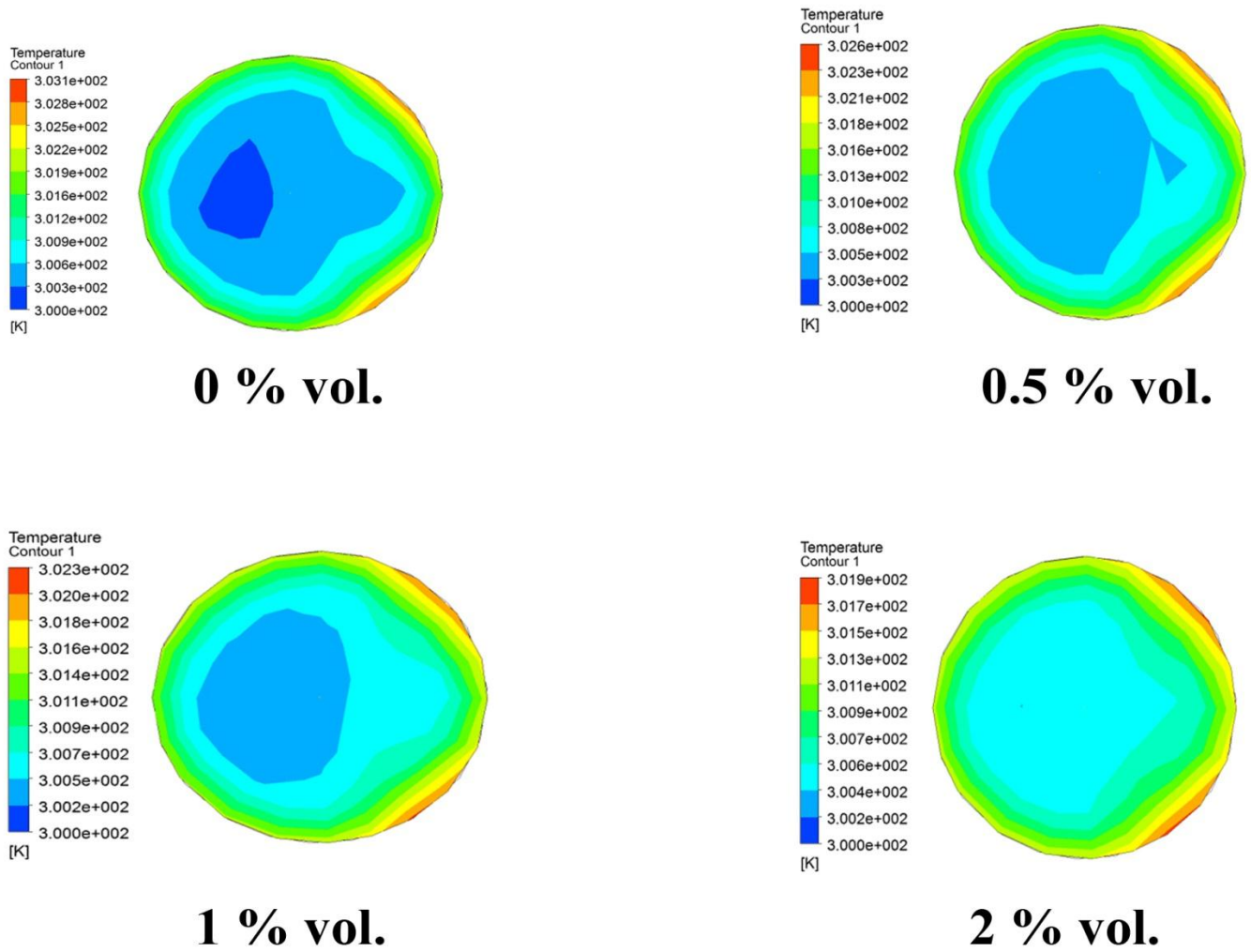
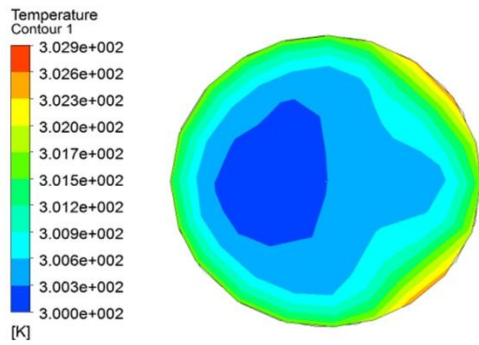
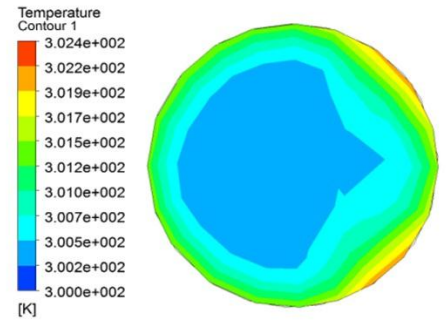


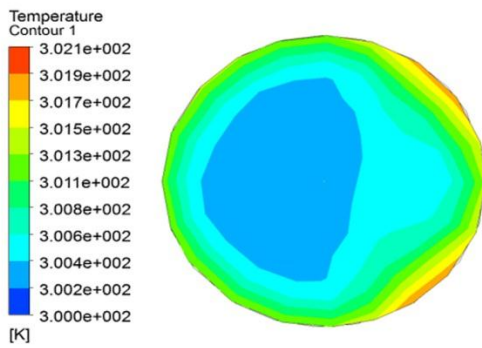
Figure 5.9: Temperature contour at outlet for  $Re = 1700$



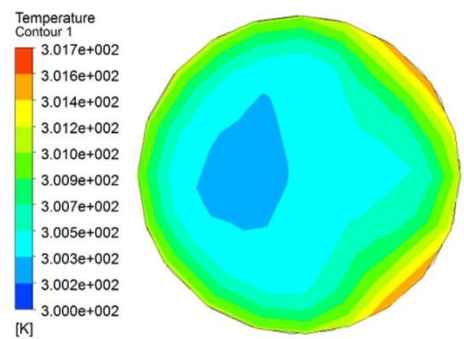
**0 % vol.**



**0.5 % vol.**



**1 % vol.**



**2 % vol.**

Figure 5.10: Temperature contour at outlet for  $Re = 2000$

## Heat Transfer :

Heat transfer calculations were made for different volume concentration of nanofluid by applying a constant temperature to the inlet of the channel and a constant uniform heat flux on the wall along the subchannel. In this study the average heat transfer coefficient was calculated from the equation no. (15). The average heat transfer coefficient for all the concentrations and considered Re is reported in Table 13. It is Noticed that, the useful contribution to the heat transfer provided by the inclusion of nanoparticles in comparison to the case with just the base fluid. Also note that heat transfer increases with the particles volume concentration and Re. The highest heat transfer rates are identified, for each concentration, at the highest Re. for instance, at  $Re = 2000$ , convective heat transfer coefficient of water and nanofluid containing 2 % Vol. of  $Al_2O_3$  was observed 233.46 and 596.95, respectively. Which results in 156% higher convective heat transfer coefficient of nanofluid than water . Enhancement of heat transfer coefficient of nanofluid as compared to pure water for 2 % Vol. of  $Al_2O_3$  particle at Reynolds number 2000 is given in the table . The observed increase in heat transfer coefficient could be attributed to improved thermophysical properties of the mixture with respect to the base fluid. Thus, a nanofluid with higher thermal conductivity increases the heat transfer along the channel. However, from the table 5.1, 5.2, 5.3, 5.4 and 5.5 it is observed that the difference between the wall and bulk temperatures decreases with respect to the case of the base fluid provoking the increase of the heat transfer coefficient.

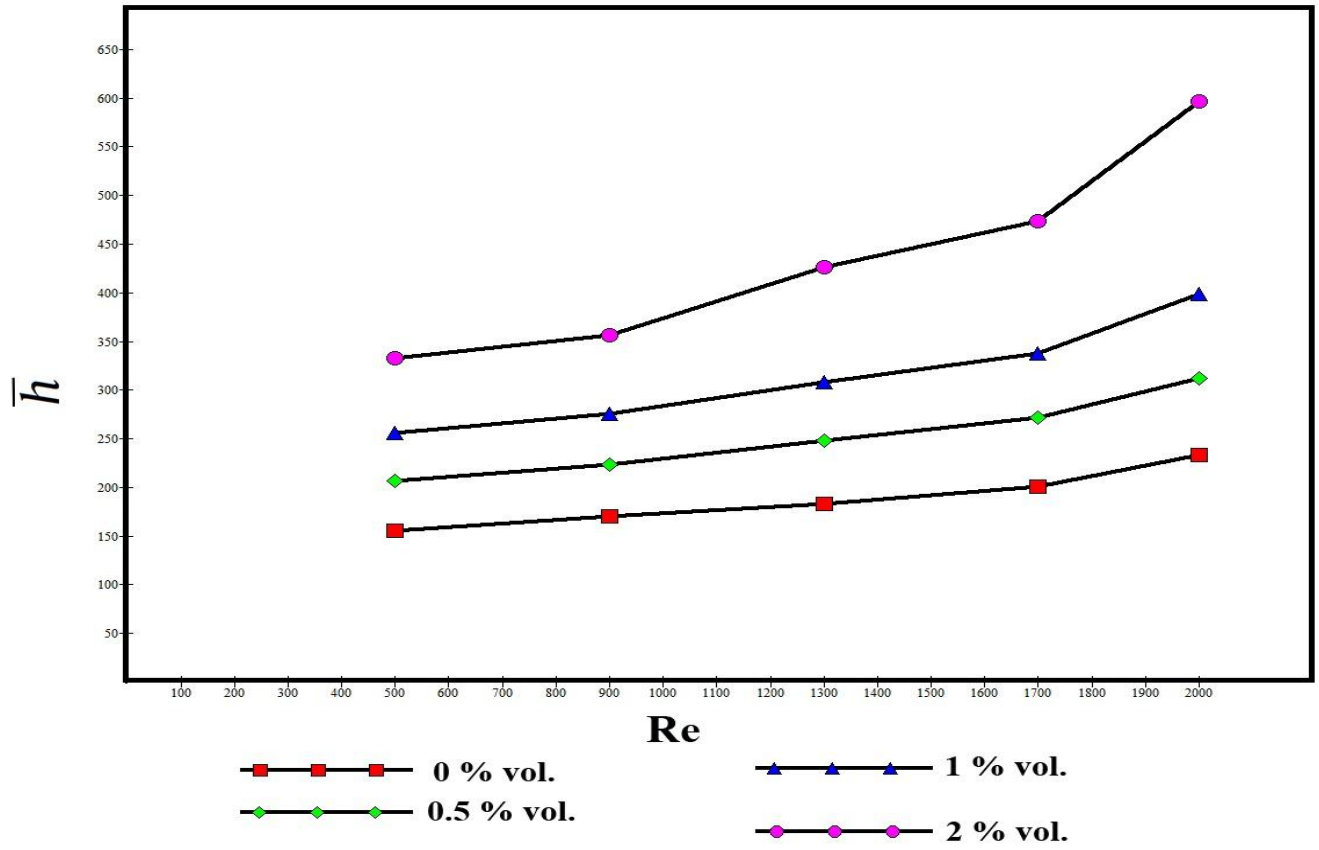


Figure 5.11: The effect of nanoparticle concentration on heat transfer coefficient

Moraveji *et al.* [21] simulated water- $\text{Al}_2\text{O}_3$  nanofluid through a tube under constant heat flux. They found that the heat transfer coefficient increased by increasing the nanoparticle concentration and Reynolds number. In this simulation we have find a similar result.

The enhancement of heat transfer coefficient of nanofluid for 2 % volume concentration and varying Reynolds number are given in the table

Table 5.15: Enhancement of Heat Transfer Coefficient

volume concentration (%)	Enhancement of Heat Transfer Coefficient (%)				
	Re = 500	Re = 900	Re = 1300	Re = 1700	Re = 2000
2	113	110	133	135	156

## Nusselt Number :

Nusselt number is the ratio of convective to conductive heat transfer across the boundary layer[23]. Named after Wilhelm Nusselt, it is a dimensionless number. It provides a comparison rate for how fast heat is transferred between materials where convection is taking place, or a flow of a gas or liquid, as compared to basic heat transfer by conduction. So the Nusselt number is often used to measure heat transfer in fluids.

Using the table 5.14 the plot of Nu vs Re at different volume concentration was obtained

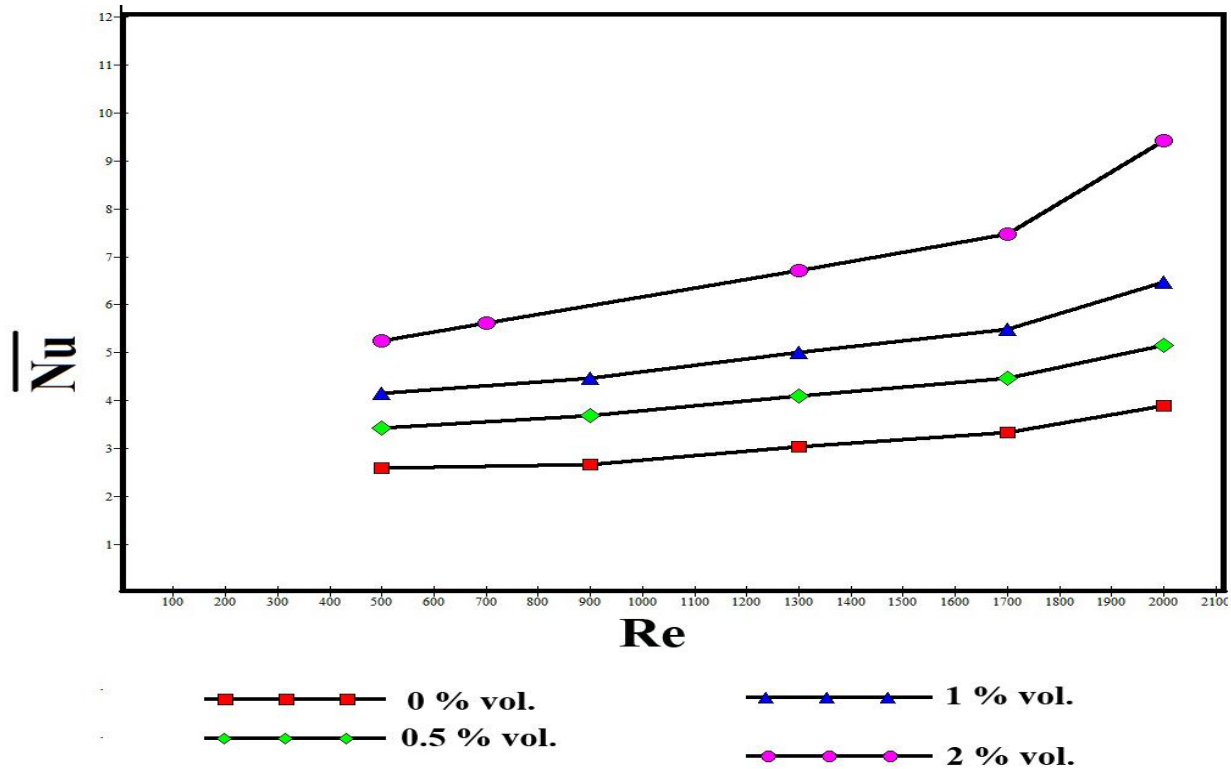


Figure 5.12: Average Nusselt number for nanofluid in different Reynolds and volume concentrations for 40 nm nanoparticle size.

Nusselt number of pure water at  $Re = 2000$  was observed 3.89 and for 2 % nanofluid containing 2 % Vol. of  $Al_2O_3$  was 7.48.

To compare the effect of applying nanoparticles in base fluid (water), thermal performance enhancement is determined.

### Thermal Performance Enhancement

$$= \frac{\text{Nusselt No. of pure water} - \text{Nusselt No. of nanofluid}}{\text{Nusselt No. of pure water}} \times 100\%$$

For example ,enhancement in thermal performance for Re = 500 and volume concentration 2 % is 102.70. Highest enhancement in thermal performance is at Re =2000 and 2 % volume concentration which is 142%.

Table 5.16: Enhancement in Thermal Performance

volume concentration (%)	Thermal Performance Enhancement (%)				
	Re = 500	Re = 900	Re = 1300	Re = 1700	Re = 2000
2	102.70	110	121	124	142



## CONCLUSION AND FUTURE WORK

The purpose of this thesis work is to perform an analysis of how a nanofluid-based solar collector performance would compare to a conventional one. Numerical simulation has been presented on heat transfer characteristics of  $\text{Al}_2\text{O}_3$ /water nanofluid containing 40nm nanoparticles in flat plate solar collector under steady state laminar flow using ANSYS-FLUENT commercial CFD package. Two phase mixture model is used to simulate the nanofluid flow taking into account appropriate thermo-physical properties. The results of simulation showed the positive influence of nanofluid over water as a solar collector working fluid on the thermal performance of system. The convective heat transfer of nanofluid increases with increasing of nanoparticles concentration and Reynolds number . At same Reynolds number increasing the volume concentration , outlet temperature increases. Increasing of flow Reynolds number results in later formation of fully developed region and decreasing of wall temperature.

The concluded points of this work are as follows:

1. The highest enhancement in thermal performance of solar collector is 142% at Reynolds number and 2 % volume concentration .
2. At same Reynolds number increasing the volume concentration , heat absorbed by the working fluid increases.
3. The suspended nanoparticles enhance the thermal conductivity which results improvement in efficiency of heat transfer systems.
4. One of the main reasons of getting higher efficiency is the very small particle size which enhances the absorption capacity of nanofluids as mixture becomes more stable and hence, sedimentation does not occurs.
5. After a certain limit of volume concentration the thermal performance declines for nanoparticle of 50nm this limit is 4.3 % [22]
6. From the temperature contour it is seen that application of nanoparticles has Good impact on the outlet temperature

Area of application of nanofluids in solar energy is a very new research field, there are also some contradictions in the results of some research work as it is the initial phase of implementing nanofluids in solar energy. So, there is a necessity of further theoretical as well as experimental work, investigations to enhance the efficiency of solar collector and to obtain firm and

authenticate results. It can be concluded that nanofluids have a good potential in solar thermal application and nanofluid is the answer for the heat transfer limitation of conventional heat transfer fluids.

Acoustic cavitation is a very complicated physical phenomenon generated by acoustic fields in liquid. Several interesting heat transfer phenomenon occur when acoustic effect is given. Heat transfer characteristics of copper nanofluid with and without acoustic cavitation were investigated by D.W. Zhou and DENG-YING LIU[31]. The results indicated that the copper nanoparticles and acoustic cavitation had profound and significant influence on heat transfer in fluid. My future plan is to investigate the acoustic effect on the heat transfer mechanism on nanofluid using CFD simulation.

## REFERENCES

---

1. Prashant Sharma. Thermal performance of low flux solar collector using CuO-H<sub>2</sub>O based nanofluid. Mechanical Engineering Department Thapar University, Patiala
2. L. Syam Sundar, and K.V. Sharma, Laminar convective heat transfer and friction factor of nanofluid in circular tube fitted with twisted tape inserts. *International Journal of Automotive and Mechanical Engineering (IJAME)*, Volume 3, pp. 265-278, January-June 2011.
3. Shung-Wen Kang, Wei-Chiang Wei, Sheng-Hong Tsai , Shih-Yu Yang. Experimental investigation of silver nano-fluid on heat pipe thermal performance. *Applied Thermal Engineering* 26 (2006) 2377–2382.
4. Mohammad Kalteh , Abbas Abbassi , Majid Saffar-Avval , Arjan Frijns , Anton Darhuber, Jens Harting , Experimental and numerical investigation of nanofluid forced convection inside a wide microchannel heat sink. *Applied Thermal Engineering* 36 (2012) 260-268.
5. Barzin Gavtash, Khalid Hussain, Mohammad Layeghi, Saeed Sadeghi Lafmejani, Numerical Simulation of the Effects of Nanofluid on a Heat Pipe Thermal Performance. *International Journal of Mechanical and Aerospace Engineering* 6 2012
6. M.M. Heyhat and F. Kowsary, Numerical simulation of forced convection of nanofluid by a two-component nonhomogeneous model. University College of Engineering, University of Tehran
7. Vincenzo Bianco, Oronzio Manca and Sergio Nardini, Numerical Simulation of Water/Al<sub>2</sub>O<sub>3</sub> Nanofluid Turbulent Convection. Hindawi Publishing Corporation, Volume 2010, Article ID 976254, 10 pages.
8. Mohammad Kalteh , Abbas Abbassi , Majid Saffar-Avval, Jens Harting, Eulerian–Eulerian two-phase numerical simulation of nanofluid laminar forced convection in a microchannel. *International Journal of Heat and Fluid Flow* 32 (2011) 107–116.
9. M. Nuim Labib, Md. J. Nine, Handry Afrianto, Hanshik Chung, Hyomin Jeong, Numerical investigation on effect of base fluids and hybrid nanofluid in forced convective heat transfer. *International Journal of Thermal Sciences* 71 (2013) 163-171.
10. H. Demir, A.S. Dalkilic, N.A. Kürekci, W. Duangthongsuk, S. Wongwises. Numerical investigation on the single phase forced convection heat transfer characteristics of TiO<sub>2</sub> nanofluids in a double-tube counter flow heat exchanger. *International Communications in Heat and Mass Transfer* 38 (2011) 218–228.

11. Sarit k. Das, Stephen U. S. choi, Wenhua yu, T. pradeep ,NANOFLUIDS-Science and technology
12. L. Schiller, A. Naumann, A drag coefficient correlation, Z. Ver. Deutsch. Ing. 77 (1935) 318-320.
13. M. Manninen, V. Taivassalo, S. Kallio, On the mixture model for multiphase flow, Technical Research Center of Finland, 288, VTT Publications, 1996, pp. 9–18.
14. Hamilton, R.L.; Crosser , O.K. Thermal conductivity of heterogeneous two component systems.*Ind. Eng. Chem.*, **1962**, *1*, 187-191.
15. B. C. Pak and Y. I. Cho, Hydrodynamic and heat transfer study of dispersed fluids with submicron metallic oxide particles. *Experimental Heat Transfer*, vol. 11, no. 2, pp. 151–170, 1998.
16. Maiga, S.E.B.; Nguyen, C.T.; Galanis, N.; Roy, G. Heat transfer behaviours of nanofluids in a uniformly heated tube. *Superlattice Microst.*, 2004, 35,543-557.
17. Christina Raab, Myrtil Simkó\*,Ulrich Fiedeler, Michael Nentwich, André Gazsó Nano trust dossirs No. 006en, February 2011.
18. René Overney / UW,Nanothermodynamics and Nanoparticle Synthesis NME 498A / A 2010 .
19. Fluent 14.0 User Manual, Fluent Incorporated, 2006.
20. <http://www.wisegeek.com/what-is-the-nusselt-number.htm>
21. Moraveji MK, Darabi M, Hossein Haddad SM, Davarnejad R (2011) Modeling of convective heat transfer of a nanofluid in the developing region of tube flow with computational fluid dynamics. *Int Commun Heat Mass Transfer* 38:1291–1295.
22. K. Singh. Thermal Conductivity of Nanofluids. *Defence Science Journal*, Vol. 58, No. 5, September 2008, pp. 600-607.
23. <http://www.wisegeek.com/what-is-the-nusselt-number.htm>
24. [http://en.wikipedia.org/wiki/Solar\\_collector](http://en.wikipedia.org/wiki/Solar_collector)
25. <http://www.google.com.bd/url?sa=t&rct=j&q=&esrc=s&source=web&cd=1&cad=rja&ved=0CCwQFjAA&url=http%3A%2F%2Fwww.ansys.com%2Fstaticassets%2FANSYS%2FConference%2FConfidence%2FChicago%2FDownloads%2Fa-solution-for-every-multiphase->

challenge.pdf&ei=bBpkUoX0HsqxrgfApoFo&usg=AFQjCNEq2p3aFrGig4eUNqt2PPB5  
2xfCrw&bvm=bv.54934254,d.bmk

26. [http://combust.hit.edu.cn:8080/fluent/Fluent60\\_help/html/ug/node690.htm](http://combust.hit.edu.cn:8080/fluent/Fluent60_help/html/ug/node690.htm)
27. [http://combust.hit.edu.cn:8080/fluent/Fluent60\\_help/html/ug/node691.htm](http://combust.hit.edu.cn:8080/fluent/Fluent60_help/html/ug/node691.htm)
28. [http://combust.hit.edu.cn:8080/fluent/Fluent60\\_help/html/ug/node692.htm](http://combust.hit.edu.cn:8080/fluent/Fluent60_help/html/ug/node692.htm)
29. [http://combust.hit.edu.cn:8080/fluent/Fluent60\\_help/html/ug/node693.htm](http://combust.hit.edu.cn:8080/fluent/Fluent60_help/html/ug/node693.htm)
30. [http://combust.hit.edu.cn:8080/fluent/Fluent60\\_help/html/ug/node694.htm](http://combust.hit.edu.cn:8080/fluent/Fluent60_help/html/ug/node694.htm)
31. [http://www.tandfonline.com/doi/abs/10.1080/01457630490486274?journalCode=uhte20#  
preview](http://www.tandfonline.com/doi/abs/10.1080/01457630490486274?journalCode=uhte20#preview)
32. [http://en.wikipedia.org/wiki/Computational\\_fluid\\_dynamics](http://en.wikipedia.org/wiki/Computational_fluid_dynamics)

